Bark Beetle Impacts on Remotely Sensed Evapotranspiration in the Colorado Rocky Mountains

John F. Knowles
Institute of Arctic and Alpine Research, University of Colorado Boulder
School of Geography and Development, University of Arizona

Noah P. Molotoch
Institute of Arctic and Alpine Research, University of Colorado Boulder
Department of Geography, University of Colorado Boulder
Jet Propulsion Laboratory, California Institute of Technology

January 2019

CWI Completion Report No.236

Colorado State University

Acknowledgements

Special thanks to Andrew Badger, Max Berkelhammer, John Frank, Leanne Lestak, Ben Livneh, and the University of Colorado Center for Water, Earth Science, and Technology (CWEST) for helping to make this work possible. The authors acknowledge financial support from the Colorado Water Institute through the project "Bark beetle impacts on remotely sensed evapotranspiration in the Colorado Rocky Mountains" (CWCB Award #5365761). The MODIS Leaf Area Index/FPAR 8-Day version 6 data product was retrieved from the online Data Pool, courtesy of the NASA Land Processes Distributed Active Archive Center (LP DAAC), USGS/Earth Resources Observation and Science (EROS) Center, Sioux Falls, South Dakota (https://lpdaac.usgs.gov/data_access/data_pool).

This report was financed in part by the U.S. Department of the Interior, Geological Survey, through the Colorado Water Institute. The views and conclusions contained in this document are those of the authors and should not be interpreted as necessarily representing the official policies, either expressed or implied, of the U.S. Government.

Additional copies of this report can be obtained from the Colorado Water Institute, E102 Engineering Building, Colorado State University, Fort Collins, CO 80523-1033 970-491-6308 or email: cwi@colostate.edu, or downloaded as a PDF file from http://www.cwi.colostate.edu.

Abstract:

Bark beetles represent a major ongoing forest disturbance throughout the southern Rocky Mountains with unknown implications for hydrological partitioning between the abiotic (evaporation) and biotic (transpiration) components of the total evapotranspiration (ET) flux. Since changes in ET are linked to both groundwater and surface water recharge processes, this scenario has the potential to affect water delivery to agricultural, industrial, and residential consumers downstream. Accordingly, this research used satellite remote sensing, eddy covariance, and hydrological modeling approaches to independently quantify the impact of bark beetles on growing season ET, the transpiration fraction of ET (T/ET), and streamflow across a range of spatial scales throughout the 144,462 km^2 EPA Level III Southern Rocky Mountain ecoregion. The results of this work demonstrate statistically significant post-disturbance ET reductions between 9% (remote sensing) and 28% (eddy covariance) relative to pre-disturbance conditions. Further, commensurate decreases in transpiration and T/ET from disturbed areas suggest that the total ET flux was primarily sensitive to changes in transpiration. In the context of the water balance, the Variable Infiltration Capacity (VIC) hydrological model simulated decreased canopy interception and increased soil moisture as a result of beetle disturbance, which increased streamflow by 9%. Factoring in the number of grid cells that were disturbed, bark beetles decreased ET by 62,000 acre-feet and increased streamflow by 54,000 acre-feet between 2000 and 2013. These results will benefit water managers tasked with forecasting water resources from disturbed areas both now and in the future.

Keywords: Evapotranspiration; Partitioning; Streamflow; Bark beetles; Remote sensing; Eddy covariance; Hydrological model; Rocky Mountains

Table of Contents:

List of Figures

I. JUSTIFICATION OF WORK PERFORMED

Evapotranspiration (ET) regulates both surface water and groundwater recharge and is thus critically important to water resources (Maxwell & Condon, 2016; Ukkola et al., 2015). However, ET is a major unknown is most hydrological systems due to spatio-temporally variable controls on the abiotic surface evaporation (E) and biotic transpiration (T) components of the total ET flux e.g. (Kool et al., 2014), particularly in the mountains where ET has been identified as a research priority (Viviroli et al., 2011). Moreover, changes in land cover complicate hydrological forecast models by potentially altering hydrological partitioning between E and T and further between ET and streamflow (Huxman et al., 2005; Sterling, Ducharne, & Polcher, 2012). In Colorado and throughout the southern Rocky Mountains, vegetation mortality due to bark beetles represents a major ongoing forest disturbance (Hicke et al. 2012; Colorado State Forest Service, 2017), but the aggregated effect of bark beetles on E and T is not well understood. As a result, this study utilized a multi-scale research design that incorporated three independent ET datasets and two methods to partition T from E, in order to constrain the links between bark beetle disturbance and ET in mountain areas that are disproportionately important to water resources.

The specific goals of this work were to (1) quantify the net effect of bark beetles on ET and the transpiration fraction of ET (T/ET) and (2) evaluate this impact within the context of the water balance throughout the EPA Level III Southern Rocky Mountain ecoregion. **Our original hypothesis was that transpiration would decrease but evaporation would increase as a result of epidemic bark beetle populations with a net negative effect on total ET.** To achieve this, we used a combination of satellite remote sensing, eddy covariance, and hydrological modeling approaches. We then leveraged the hydrological model to contextualize our results

within the regional water balance. These analyses ultimately yielded methodological consensus that **bark beetles had a singularly negative effect on both ET and T/ET; we observed no significant evidence of a compensating physical evaporation response to decreased transpiration. Further, our modeling analysis demonstrated that reduced ET fluxes in the beetle simulation were generally partitioned to increased streamflow.** This project achieved all of its goals as originally stated, and we believe this work will be useful to both hydrological forecast modelers and water managers seeking to quantitatively evaluate the impact of land cover change due to bark beetles on evapotranspiration and streamflow.

II. REVIEW OF METHODS USED

Remote Sensing

The remote sensing component of this study focused on areas within the 144,462 km^2 Southern Rocky Mountain ecoregion (SRME; Commission for Environmental Cooperation, 1997; United States Environmental Protection Agency, 2010) located a1,500 meters above sea level (Figure 1). Analyses were masked to include only areas with evergreen forests as determined by the Landsat-based U.S. Geological Survey (USGS) 2001 National Land Cover Database (NLCD) data (http://www.mrlc.gov/nlcd2001.php; Homer et al., 2004). The NLCD data were upscaled from 30 m to 1 km cell size for consistency with the remotely sensed ET data from the Moderate Resolution Imaging Spectroradiometer (MODIS). Aggregation to 1 km resolution was performed based on the percentage of 30 m evergreen cells inside each 1 km grid cell such that the resulting evergreen mask contained only areas with greater than 50% evergreen forest cover. Principal tree species (from approximately north to south) included Engelmann spruce (*Picea engelmanii*), subalpine fir (*Abies lasioscarpa*), lodgepole pine (*Pinus contorta*), limber pine (*Pinus flexilis*),

Douglas fir (*Pseudotsuga menziesii*), blue spruce (*Picea pungens*), white fir (*Abies concolor*), ponderosa pine (*Pinus ponderosa*), and southwestern white pine (*Pinus strobiformis*). Additionally, we utilized the United States Forest Service (USFS) Aerial Detection Survey (ADS) data to select two smaller focus areas consisting of contiguous or nearly contiguous polygons that experienced exceptional vegetation mortality due to bark beetles (Figure 1). The latitude and longitude at the centers of Focus Areas 1 (301 km^2) and 2 (168 km^2) were 40º52.5' N; 106º4.3' W and 40º3.8' N; 106º37.1' W, respectively, and the elevation within each focus area ranged from 2,500 to 3,200 meters above sea level.

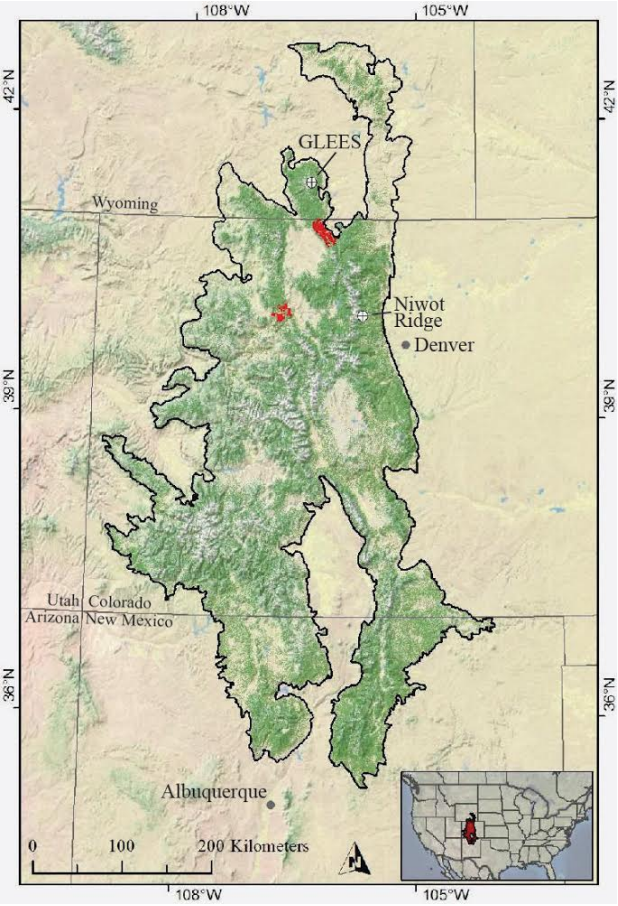

Figure 1. Site map shows evergreen forests above 1,500 meters elevation as green areas and two focus areas that were used to constrain the effects of disturbance as red areas. The black outline is the boundary of the Southern Rocky Mountain ecoregion.

Monthly MODIS-based estimates of ET at 1 km resolution were generated by temporal averaging of the MODIS 8-day ET data products (MOD16A2; Running et al., 2017; Mu et al., 2011). The ET estimates were based on the Penman-Monteith equation forced by both ancillary meteorological data and 8-day MODIS-based vegetation information. The MODIS ET product is generated using four MODIS-based data sources including 8-day composites of Fractional Absorbed Photosynthetically Active Radiation (FPAR), 8-day land surface albedo, 8-day Leaf Area Index (LAI), and land cover type. The 8-day albedo composites were combined with daily surface solar irradiance and air temperature data from meteorological reanalysis to derive the surface net radiation and ground heat flux (Mu et al., 2011). Surface stomatal conductance and aerodynamic resistance were estimated from a combination of MODIS LAI and reanalysis of daily air temperature, vapor pressure deficit, and relative humidity. Biome-dependent vegetation parameters were obtained from MODIS-based land cover information. These parameters were optimized such that annual ET estimates for each biome agreed with ET estimates based on MODIS-derived Gross Primary Productivity (GPP) and known water use efficiencies established from eddy covariance measurements (Mu et al., 2011).

Areas of disturbance were identified, and disturbance masks were created, using the USFS ADS data. The USFS Aerial Detection Surveys estimated forest mortality based on manual observations from aircraft wherein visual estimates of dead trees were obtained and transcribed manually onto a base map. When converting the polygons from vector to raster format, only raster cells containing more than 70% coverage of mortality polygons were included in the disturbance mask. In this way, the ADS data were used only as an index of the presence/absence of disturbance. When relative differences in vegetation mortality were considered (e.g., the focus area analysis), a standardized (for host species type and crown area)

ADS product was used (Meddens et al., 2012). The year of forest mortality was estimated by subtracting one year from the survey date. This 1-year subtraction was necessary given that trees are in the red phase when they are detected and therefore represent the year after initial mortality. Ecoregion-scale disturbance masks remained spatially fixed at the maximum and minimum extents of disturbed and undisturbed areas, respectively, which occurred in 2014. In this way, disturbed areas experienced progressively more mortality through time, which when compared to undisturbed areas on an interannual basis, allows for calculation of the disturbance impact and separation of the relative climatic versus disturbance influences on ET. Mean MODIS ET for each disturbance mask was calculated using the ArcGIS zonal statistics function.

Eddy Covariance

Methodological Description

Airflow near Earth's surface contains variably-sized rotating eddies, each of which possesses three-dimensional components (e.g. Oke 1987). These eddies constantly move parcels of air with measurable concentrations of trace gases and kinetic energy up and down throughout the turbulent surface layer of Earth's atmosphere. Accordingly, the eddy covariance method uses fast response sensors mounted above the vegetation canopy to quantify the mean covariance between instantaneous deviations in vertical wind speed and various scalars contained within the parcel of air being transported including momentum, heat, and trace gases including water vapor (e.g. Aubinet et al., 2000; Baldocchi et al., 2001). In this way, the eddy covariance method provides a continuous measurement of surface-atmosphere flux within a statistical footprint that generally ranges from 1-2 km upwind. This study used eddy covariance measurements of surface-atmosphere water vapor exchange to quantify evapotranspiration dynamics at two locations

within the Southern Rocky Mountain ecoregion, one of which (the Glacier Lakes Ecosystem Experiments Site) was significantly affected by bark beetles during the study period.

Glacier Lakes Ecosystem Experiments Site

The Glacier Lakes Ecosystem Experiments Site (GLEES) is located west of Laramie, Wyoming, USA at an elevation of 3190 meters above sea level in the Snowy Range Mountains (41°21.992' N; 106°14.397' W) (Frank, Massman, Ewers, Huckaby, & Negron, 2014; Speckman et al., 2014). Continuous, ongoing eddy covariance data collection began in October 2004 (U.S. Department of Energy AmeriFlux ID = US-GLE), and the long-term mean annual air temperature and precipitation are -2 °C and 1200 mm, respectively. The subalpine forest at this location is comprised of Engelmann spruce and subalpine fir, with an average canopy height of 18 m. Since 2007, the forest has experienced has experienced an outbreak of spruce bark beetle (*Dendroctonus rufipennis*) due to a lack of wintertime low air temperatures below the spruce beetle freeze tolerance threshold (Frank et al., 2014). As a result, healthy tree basal area has decreased from 65 m^2 ha^{-1} in 2003 to <10 m^2 ha^{-1} in 2012 (Speckman et al., 2014) (Figure 2). Eddy covariance data collection and processing details can be found in Frank et al. 2014.

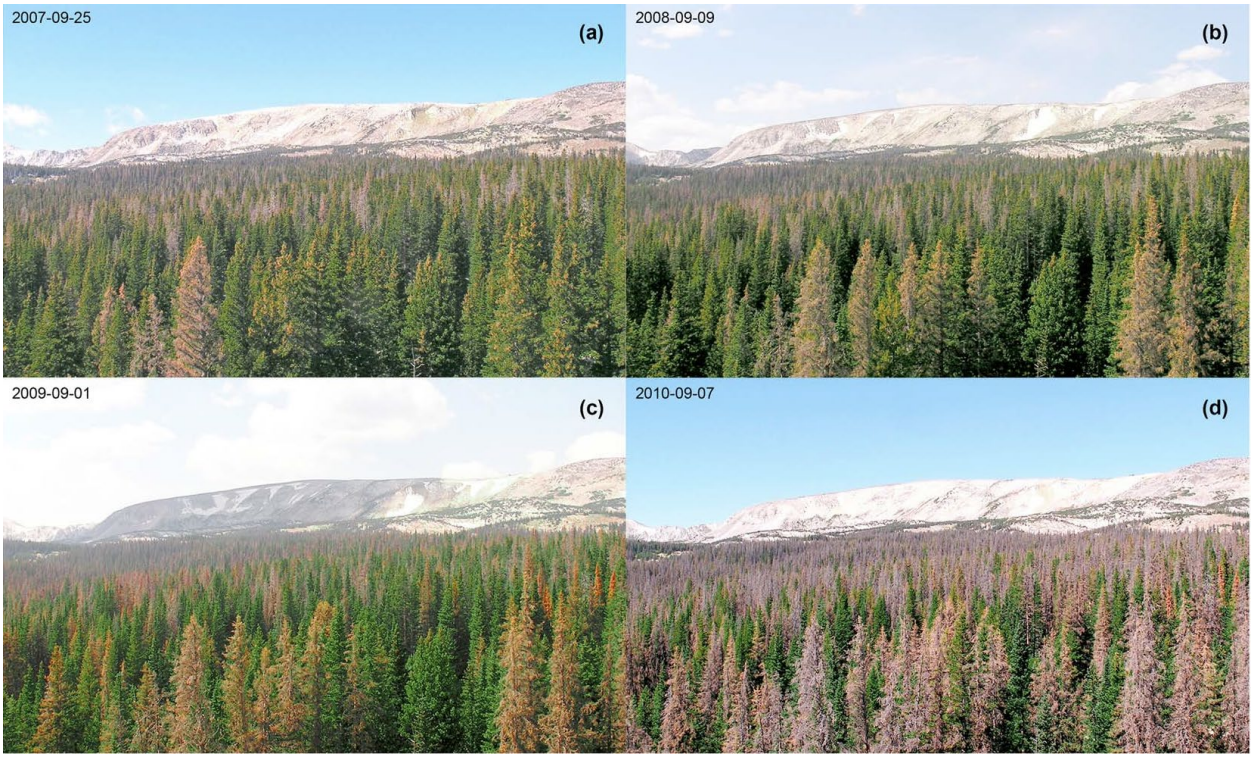

Figure 2. Repeat photography from the Glacier Lakes Ecosystem Experiments Site (GLEES) tower scaffold shows the progression of the spruce bark beetle from endemic to epidemic populations (photos originally published in Frank et al. 2014).

Niwot Ridge Site

The Niwot Ridge AmeriFlux (ID = US-NR1) tower is located in the subalpine forest approximately 25 km west of Boulder, Colorado, USA and 8 km east of the Continental Divide at 3050 meters above sea level (40º1'58.4" N; 105º32'47.0" W). Continuous, ongoing eddy covariance data collection began at this location in November 1998, and the long-term mean annual air temperature and precipitation are 1.3 ºC and 698 mm, respectively (Knowles, Burns, Blanken, & Monson, 2015a), which make it warmer and drier than the GLEES site. The mixed coniferous forest consists of lodgepole pine, subalpine fir, and Engelmann spruce, and the mean canopy height was 11.5 m in 2002 (Turnipseed, Blanken, Anderson, & Monson, 2002). Although bark beetles are endemic to this location, less than 6% of the trees around the tower were affected by beetles in 2013 (Moore et al., 2013; Figure 3); therefore, we used this site as a

control with which to establish the effect of beetles on ET and the transpiration fraction of ET (T/ET). Additional specifics about the instrumentation, data collection, and processing at Niwot Ridge can be found in Burns et al. 2016.

Figure 3. Photograph from the Niwot Ridge AmeriFlux tower looking west toward the Continental Divide (J. Knowles, September 2013).

Transpiration partitioning

The transpiration fraction of ET was determined using an "optimal approach" (Berkelhammer et al., 2016) that assumes close correlation between rates of ecosystem transpiration and gross primary production (GPP), i.e. the stomatal-driven components of an ecosystem's water and carbon fluxes derived from eddy covariance data. At both the GLEES and Niwot Ridge sites, the GPP was modeled from direct measurements of the net ecosystem exchange of carbon dioxide

(NEE) using a soil temperature response function to extrapolate nighttime carbon dioxide respiration values throughout the daytime hours (Reichstein et al., 2005). Both ET and GPP were subsequently normalized by vapor pressure deficit (VPD), which linearizes the relationship between ET and GPP and is analogous to water use efficiency (Beer et al., 2009; Zhou, Yu, Huang, & Wang, 2014), and a second-order power law function was used to describe the relationship between the 5^{th} percentile of ET and normalized, binned GPP (Berkelhammer et al., 2016). The 5^{th} percentile of ET was used in favor of the minimum ET because the singular ET minimum within a bin is often an outlier resultant from noise or bias in the gas analyzer or uncertainty in the model used to derive GPP from NEE (Berkelhammer et al., 2016). In this way, ET in excess of the minimum value within each bin must be associated with the abiotic component of the latent heat flux, i.e. evaporation from bare soil or leaf surfaces. For data quality purposes, the T/ET analysis was restricted to midday (incoming solar radiation > 600 W m^{-2}), well-mixed (friction velocity > 0.1 m s^{-1}) conditions during the growing season (1 May – 30 Sep).

Hydrological Model

The Variable Infiltration Capacity (VIC; Liang et al., 1994) land surface model is a physically based model that is able to reconcile spatio-temporally dynamic processes in complex terrain (Nijssen et al., 1997, 2001). The VIC model additionally includes mosaic land cover to capture sub-grid variability in vegetation classes, an important element in this study with which to aid representation of sub-grid variability in vegetation mortality. Within VIC, the Penman-Monteith potential evapotranspiration (Monteith, 1973) was used to dynamically compute evapotranspiration based on stomatal and architectural vegetation resistance terms. To represent

the effect of bark beetles, two changes were made to the vegetation within each disturbed grid cell in this study: (1) stomatal resistance was increased from 150 s/m (VIC default) to 305 s/m (Frank et al., 2014) and (2) leaf-area index (LAI) was reduced based on the long-term observed LAI in disturbed regions (Myneni et al., 2015; Figure 4).

This research constructed VIC on a 1/16° (~6 km) spatial grid with soil parameters derived from Livneh et al. (2013; 2015). The VIC simulations were forced by the observed meteorological dataset from Livneh et al. (2015), which is a gridded meteorological dataset that spans 64 years from 1950 to 2013; the period 1 October 1999 to 30 September 2013 was used for the modeling analysis in this study. A model spin-up simulation was performed from 1 January 1950 to 30 September 1999, with the final iteration saved as the initial condition for a series of annual water-year simulations that were run to represent vegetation changes due to bark beetle impacts from 1 October 1999 through 30 September 2013. The model state at the end of each respective water-year was used as the initial condition for the subsequent water-year.

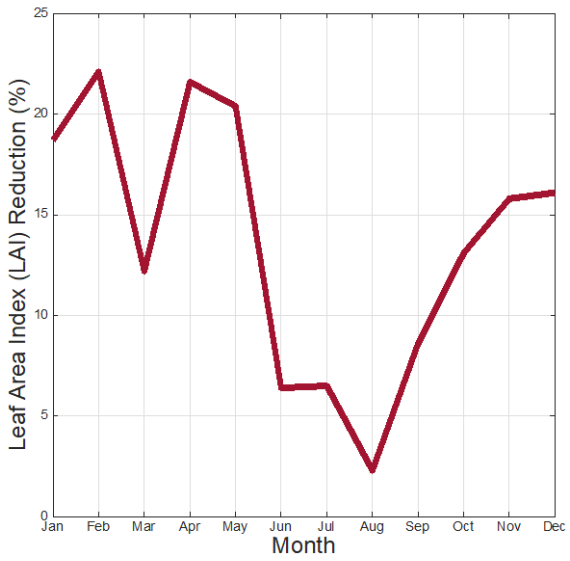

Figure 4. Monthly leaf area index (LAI) reductions that were applied to simulate beetle disturbance in model simulations (Myneni et al., 2015).

III. DISCUSSION OF RESULTS AND THEIR SIGNIFICANCE

Remote Sensing

The area of bark beetle disturbance within the Southern Rocky Mountain ecoregion increased by an order of magnitude from 2,252 km^2 in 2000 to 21,456 km^2 in 2014. Of that area, 14,499 km^2 were affected by Mountain pine bark beetle (*Dendroctonus ponderosae*), 6,122 km^2 were affected by spruce beetle, and 835 km^2 were affected by both spruce and pine beetle. An additional 1,114 km^2 land area (excluded from this study) was affected by fire as well bark beetles during the study period. Figure 5 shows the cumulative spatial extent of the bark beetle outbreak within the Southern Rocky Mountain ecoregion. Areas of bark beetle disturbance primarily occurred throughout the northern half of the study domain. The largest single-year increase in disturbance occurred between 2005 and 2006, when 3,001 new km^2 were disturbed, which represented a 46% increase in affected area from the previous year.

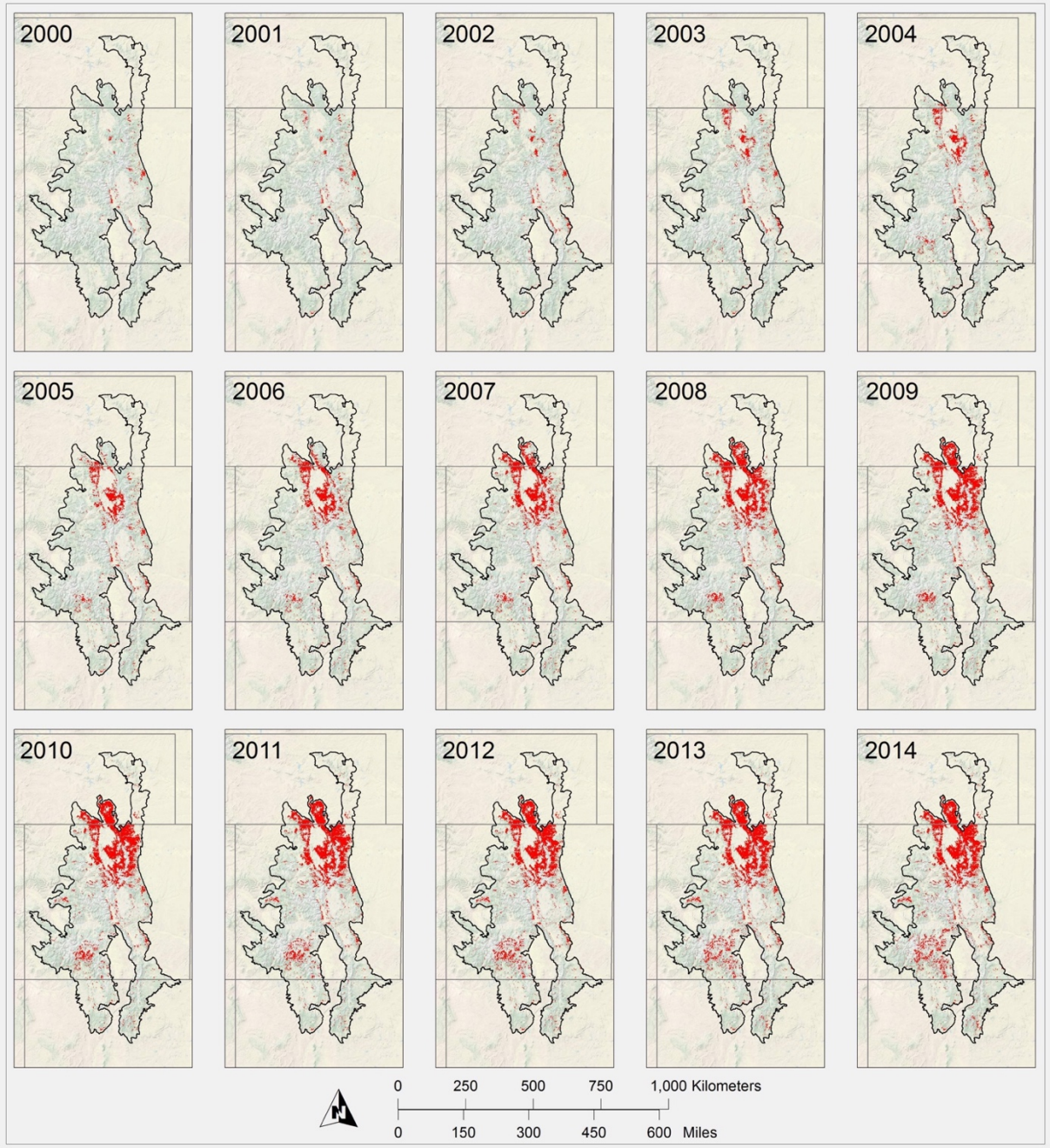

Figure 5. Cumulative annual areal extent of remotely sensed pixels identified as disturbed by bark beetles using a 70% vegetation mortality threshold.

The mean MODIS ET was 212 mm between 2000 and 2014. The ET was generally greatest on the western slope of the Continental Divide and least in the lower elevation valleys throughout the central portion of the study domain (Figure 6). Analysis of the spatially distributed anomaly from the mean annual ET illustrates the heterogeneity associated with

interactions between synoptic meteorology, topography, and disturbance throughout the study area (Figure 7). Annually, the highest and lowest mean ET were associated with large scale climate processes e.g., the ET minima coincided with regional drought in 2002 (ET = 167 mm) and 2012 (ET = 175 mm), and the maximum ET occurred in 2007 (237 mm) during a warm phase of the EL Niño Southern Oscillation (ENSO). During climatically moderate periods, the ET was increasingly influenced by local ecohydrological variability (e.g., 2001, 2003, 2013). Beginning in 2006, areas of persistently depressed ET are evident throughout the northern portion of the study domain where bark beetles reached epidemic populations.

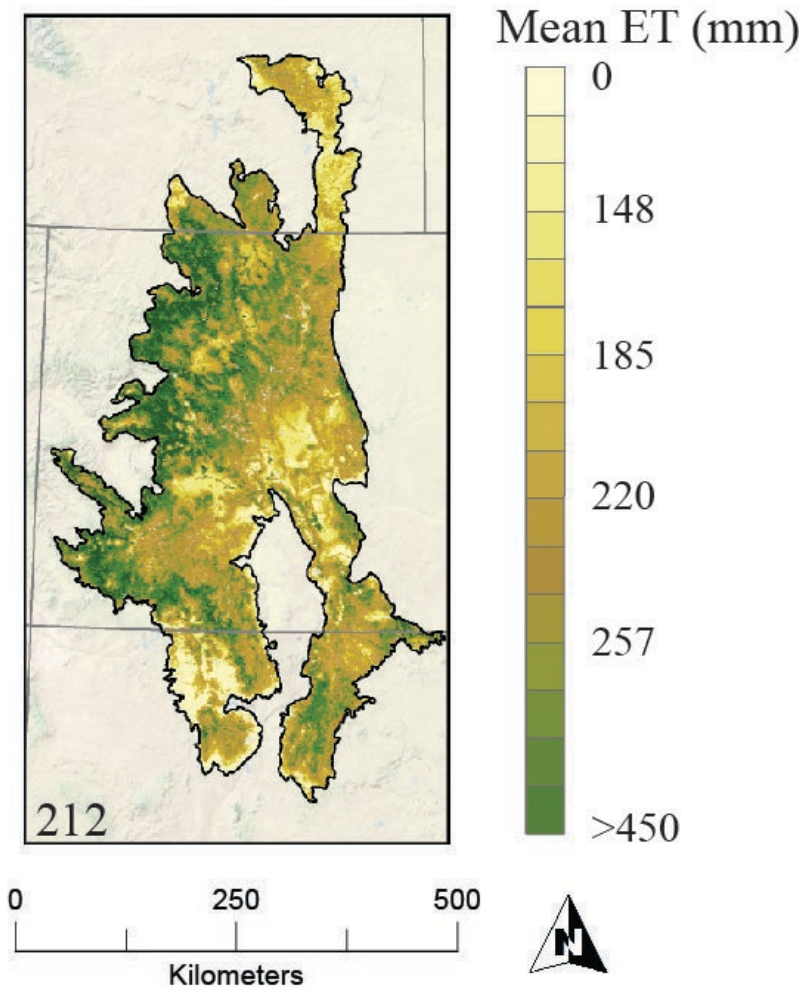

Figure 6. Spatial variability of the mean evapotranspiration (ET) throughout the Southern Rocky Mountain ecoregion between 2000 and 2014. The mean ET was 212 mm over all 15 years.

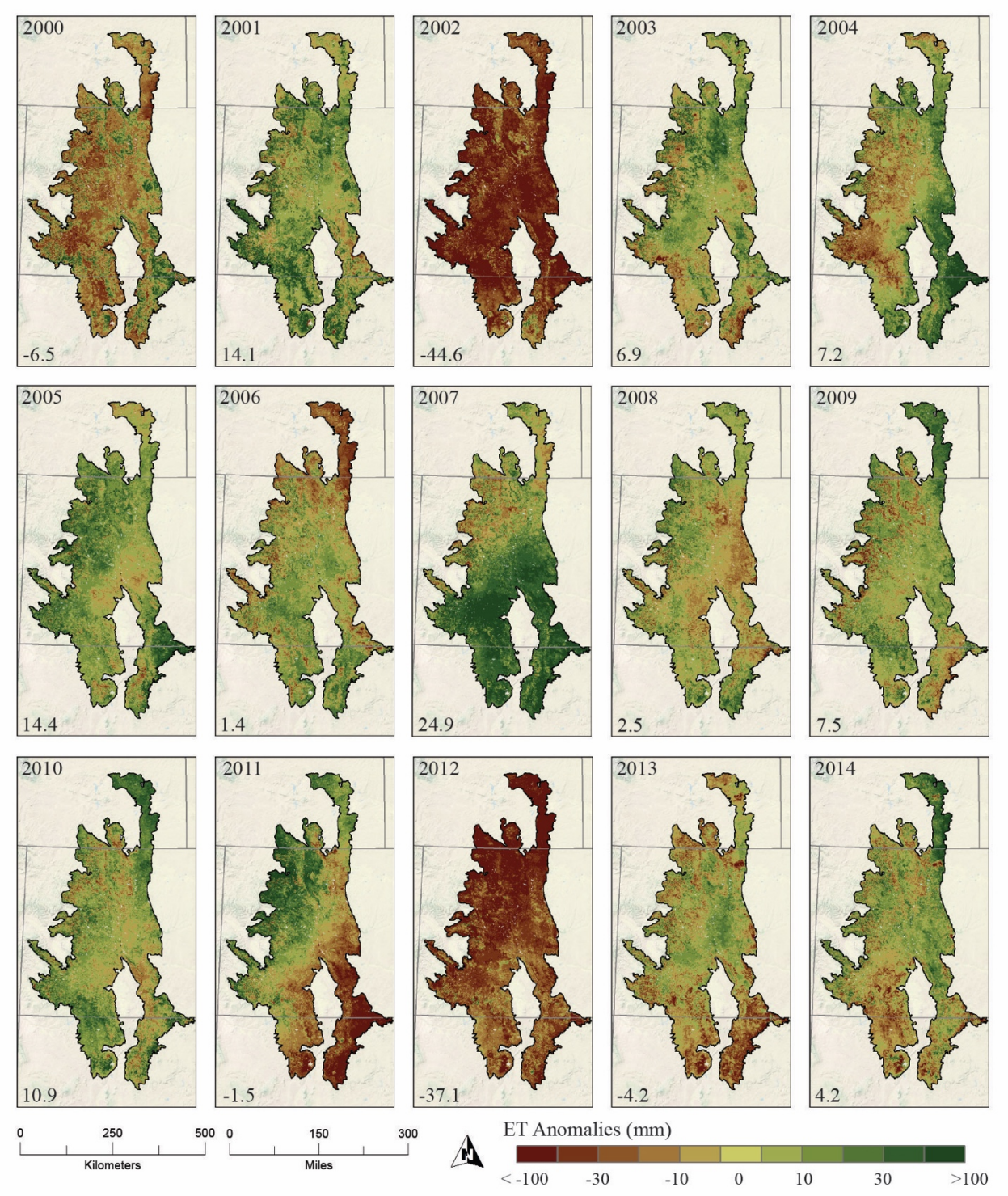

Figure 7. Spatial analysis of the annual anomaly (spatially integrated value in the lower left corner of each panel) from the 2000-2014 mean evapotranspiration (ET).

Comparison of ET from undisturbed and progressively disturbed areas through time normalizes the effect of meteorological variability and constrains the magnitude of the bark

beetle effect on vegetation. Considering a 14,572 km^2 area that experienced a minimum of 70% vegetation mortality throughout the study period, there was a significant ($p = 0.02$) decreasing ET trend between 2000 and 2014 (Figure 8a). From the slope of the Mann-Kendall regression (-1.4 mm/yr), annual growing season ET decreased from 240 mm to 220 mm (9%) in this area. There was no corresponding trend in a 38,200 km^2 relatively undisturbed area during the same time. Further, there was significantly less difference between the ET from disturbed and undisturbed areas through time (Figure 8b). Using multiple linear regression analysis, both the undisturbed ET ($p < 0.001$) and a binary disturbance metric ($p = 0.005$) were significant predictors of the mean annual ET from disturbed areas; however, the corresponding interaction term was not significant, suggesting that the sensitivity of ET to meteorological variability did not change post-disturbance. That the ET was higher to begin with in pixels that were eventually disturbed could indicate a particular forest composition or structure characteristic that favored beetle infestation in those areas (Raffa et al., 2008).

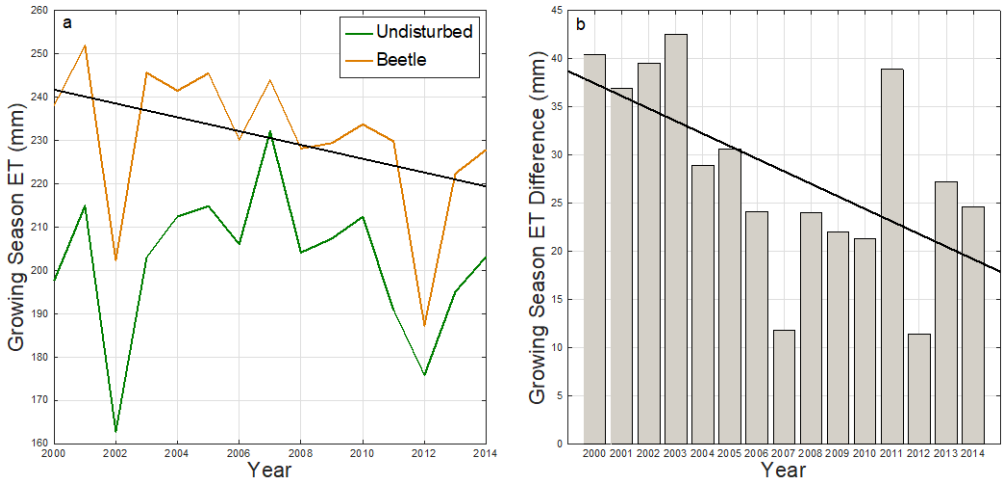

Figure 8. (a) There was a significant (Mann-Kendall $p = 0.02$) decreasing trend in growing season (1 Apr – 30 Sep) evapotranspiration (ET) from areas disturbed by bark beetle throughout the study period. There was no corresponding trend in undisturbed areas. (b) During the same time, the difference between growing season ET from undisturbed and beetle disturbed areas also decreased significantly (Mann-Kendall $p = 0.02$). Solid black lines denote significant regressions.

To further isolate beetle-induced changes in ET from those due to climatic, topographic, and/or vegetation heterogeneity, a focused analysis was conducted on two small, generally contiguous areas within the ecoregion that experienced between 83% (Focus Area 1) and 85% (Focus Area 2) vegetation mortality (Figure 9). Both focus areas experienced a significant ($0.001 < p < 0.02$) reduction in growing season ET throughout the study period (Figure 9a-b), and reduced ET was significantly ($0.02 < p < 0.06$) correlated with cumulative vegetation mortality in each case (Figure 9c-d). From the slope of the Mann-Kendall regression analyses (2.3 mm/yr), the focus area ET decreased by 13% over the 15-year time period. Alternatively, the mean focus area ET was reduced by 12% when we applied a 50% vegetation mortality threshold (i.e., restricting the analysis to pixels with greater than 50% vegetation mortality) as opposed to 11% when we applied a 70% vegetation mortality threshold (i.e., restricting the analysis to pixels with greater than 70% vegetation mortality), relative to pre-disturbance conditions.

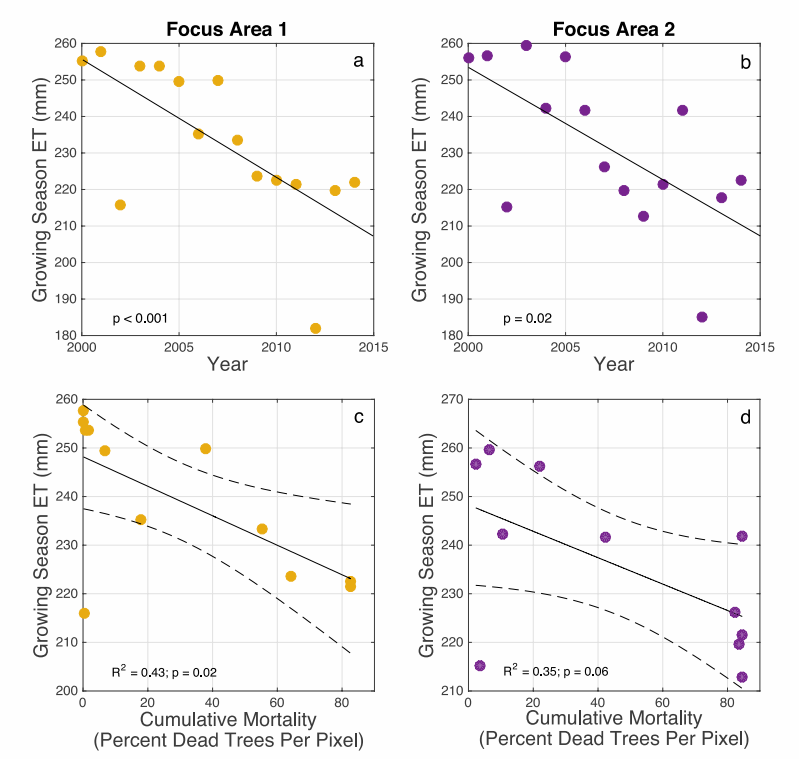

Figure 9. Analysis of two heavily disturbed focus areas within the ecoregion showed that (a, b) growing season evapotranspiration declined significantly throughout the study period (c, d) as a result of beetle-induced vegetation mortality. Solid lines denote significant relationships and dashed lines correspond to the 95% confidence interval.

Eddy Covariance

Between 2005 and 2014, the mean cumulative growing season (1 May – 30 Sep) ET at GLEES was 306 mm, or 26% of mean annual precipitation. The minimum growing season ET was 243 mm in 2011 and the maximum growing season ET was 380 mm in 2006. The spruce bark beetle outbreak at GLEES reached epidemic proportion in 2008 when more than half of impacted trees had been attacked (Frank et al., 2014), and this is reflected in the GLEES eddy covariance record (Figure 10a). The largest single-year change in the GLEES ET occurred between 2007 and 2008, during which time there was a 63 mm (17%) decrease. Overall, there was a significant ($p = 0.01$) reduction in cumulative growing season ET at GLEES throughout the 10-year period of eddy covariance data collection (Figure 10a). At Niwot Ridge, the mean cumulative growing season ET was 358 mm between 2000 and 2014, which represented 51% of mean annual precipitation. The minimum growing season ET was 314 mm in 2002, and the maximum growing season ET was 392 mm in 2013 (Figure 10b). There was no significant temporal trend in the mean annual growing season ET at Niwot Ridge.

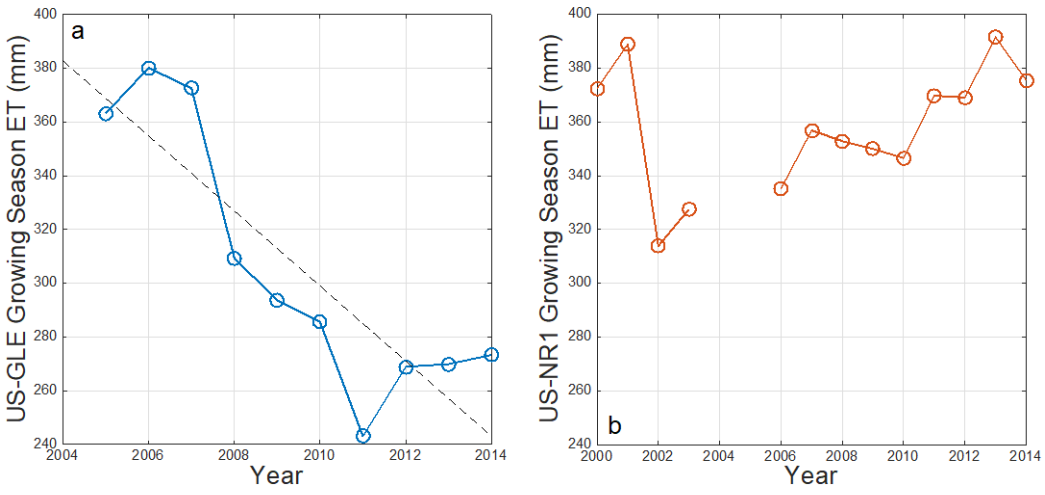

Figure 10. Cumulative annual growing season (1 May – 30 Sep) eddy covariance evapotranspiration (ET) at the (a) Glacier Lakes Ecosystem Experiments Site (US-GLE) and the (b) Niwot Ridge AmeriFlux site (US-NR1). The dashed black line shows a significant (Mann-Kendall $p = 0.01$) decreasing ET trend at US-GLE.

Comparison of the annual eddy covariance ET data from GLEES and Niwot Ridge shows a significant ($p = 0.005$) diverging trend where the GLEES ET was higher than the Niwot Ridge ET until the bark beetle epidemic in 2008, after which time the GLEES ET systematically decreased relative to Niwot Ridge (Figure 11). Accordingly, we consider the variability in the GLEES ET to result from a combination of disturbance and meteorological variability, whereas the Niwot Ridge ET primarily reflects meteorological variability. For example, there was only a 1% drop in the Niwot Ridge ET between 2007 and 2008 (when the GLEES ET dropped 17%), and the minimum ET at Niwot Ridge occurred in 2002 during the meteorological drought of record (Cook, Woodhouse, Eakin, Meko, & Stahle, 2004). As a result, Figure 11 generally removes the effect of meterological variability from the GLEES ET signal insofar as the Niwot Ridge ET is subtracted out, and we thus interpret the values in Figure 11 as an approximation of the effect of bark beetles on ET beginning in 2008. Following the classification scheme of Frank et al. 2014, the epidemic II phase at GLEES began in 2010 (impacted trees die), and Figure 11 shows a relatively stable offset between the GLEES and Niwot Ridge ET flux after that time. Specifically, our analysis suggests that between 2010 and 2014, there was an average of 102 mm (28%) less ET at GLEES relative to Niwot Ridge as result of beetle-induced tree mortality.

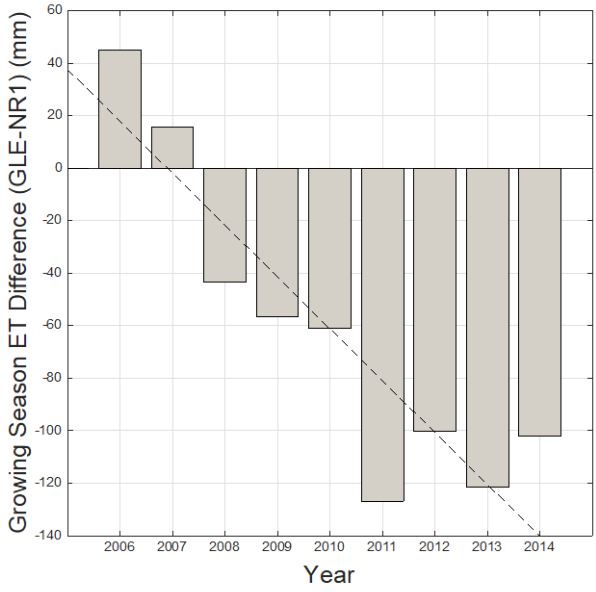

Figure 11. Annual difference in cumulative growing season (1 May – 30 Sep) eddy covariance evapotranspiration (ET) at the (a) Glacier Lakes Ecosystem Experiments Site (US-GLE) and the Niwot Ridge AmeriFlux site (US-NR1). Negative values denote less ET at US-GLE (disturbed) relative to US-NR1 (undisturbed). The dashed line shows a significant (Mann-Kendall $p = 0.005$) decreasing trend throughout the length of the simultaneous data collection record.

The transpiration component of the total growing season evapotranspiration (T/ET) averaged 0.61 at GLEES between 2005 and 2017. The minimum T/ET was 0.55 in 2014 and the maximum T/ET was 0.70 in 2007. Similar to ET, there was a significant ($p = 0.03$) decreasing trend in T/ET at GLEES throughout the study period (Figure 12a) that reduced absolute T/ET by 10% (relative T/ET by 15%) and was indicative of widespread vegetation mortality. At Niwot Ridge, the mean T/ET was 0.63 between 2000 and 2014, the minimum T/ET was 0.56 in 2010, and the maximum T/ET was 0.66 in 2006. There was no significant temporal T/ET trend at Niwot Ridge (Figure 12b). The GLEES T/ET (standard deviation = 0.044) was more variable than the Niwot Ridge T/ET (standard deviation = 0.028). In contrast to ET, there was no significant temporal pattern in the T/ET difference between GLEES and Niwot Ridge; however, this could reflect uncertainty associated with the T/ET calculation and/or the underlying GPP model.

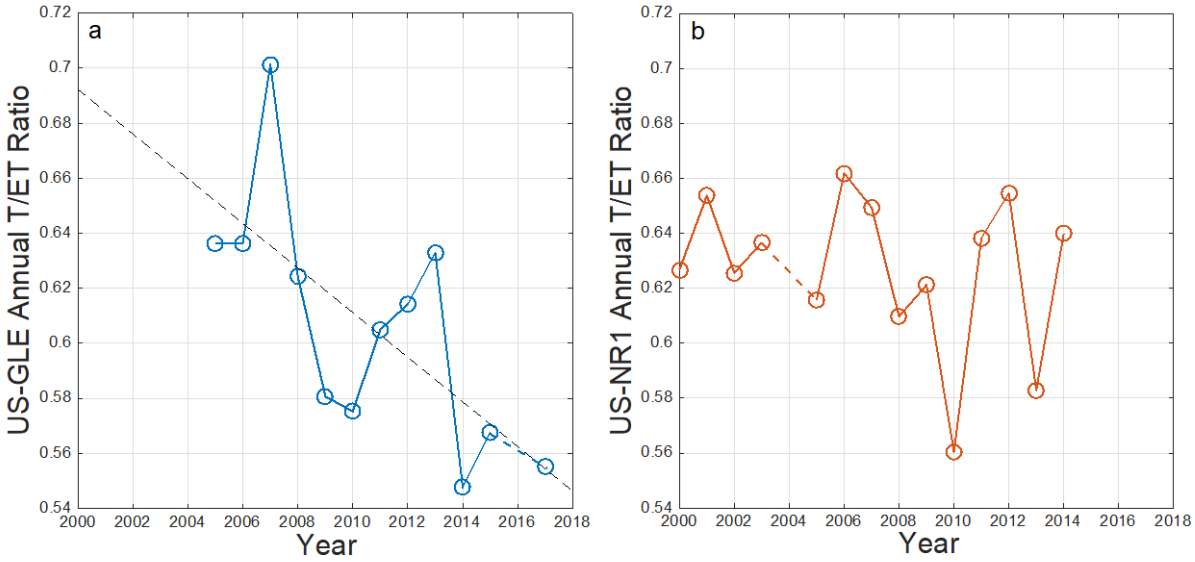

Figure 12. The annual fraction of evapotranspiration corresponding to transpiration (T/ET) at the (a) Glacier Lakes Ecosystem Experiments Site (US-GLE) sites and the (b) Niwot Ridge AmeriFlux site (US-NR1). The black dashed line denotes a significant (Mann-Kendall $p = 0.03$) decreasing T/ET trend through time at the disturbed US-GLE site. Colored dashed lines are used to connect points spanning years of missing data.

There was a significant ($p = 0.04$) relationship between cumulative growing season ET and T/ET at GLEES (Figure 13a). This indicates that decreased transpiration was a significant factor in both reduced absolute and relative (to Niwot Ridge) growing season ET at the GLEES site through time. The lack of a corresponding relationship between cumulative growing season ET and T/ET at Niwot Ridge (Figure 13b) further suggests that the interannual ET variability at Niwot Ridge was responding to complex meteorological variability in place of a singular factor or disturbance. For example, the minimum T/ET at Niwot Ridge occurred in the year with the 4th lowest ET, but the maximum T/ET occurred in the year with the 3rd lowest ET i.e., the total ET was governed by a mixture of biotic and abiotic factors to a greater degree. In sum, analysis of eddy covariance data from disturbed and control sites within the Southern Rocky Mountains ecoregion demonstrates systematically reduced ET and T/ET, and thus an overarching biotic control on total ET in the presence of disturbance.

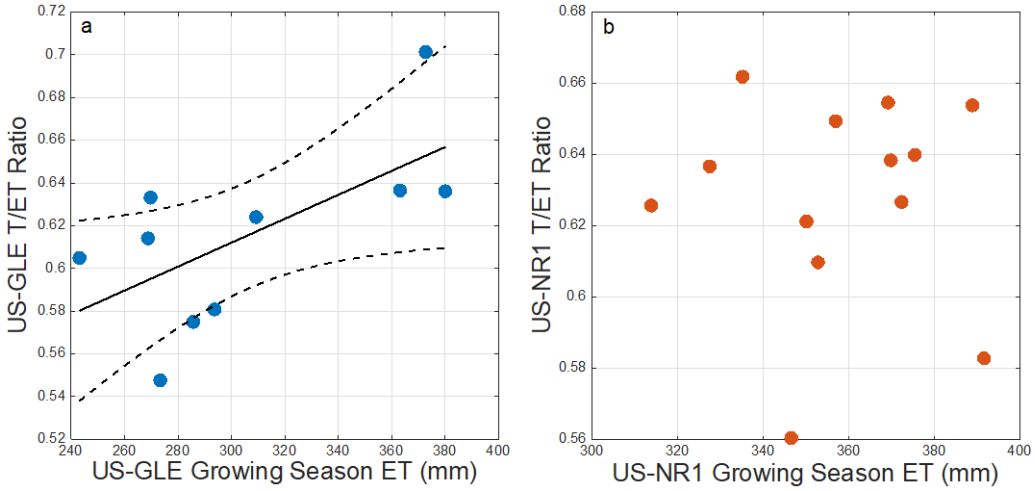

Figure 13. (a) There was a significant (p = 0.04) relationship between cumulative growing season evapotranspiration (ET) and the transpiration fraction of ET (T/ET) at the Glacier Lakes Ecosystem Experiments Site (US-GLE) but (b) not at Niwot Ridge (US-NR1). Dashed lines correspond to the 95% confidence interval.

Hydrological Model

The number of disturbed 1/16° (~36 km^2) gridboxes in the bark beetle model simulation increased from three in 2000 to 291 in 2013 (Figure 14). The largest increases occurred between 2005 and 2008, when 55 new gridboxes were disturbed in each water-year.

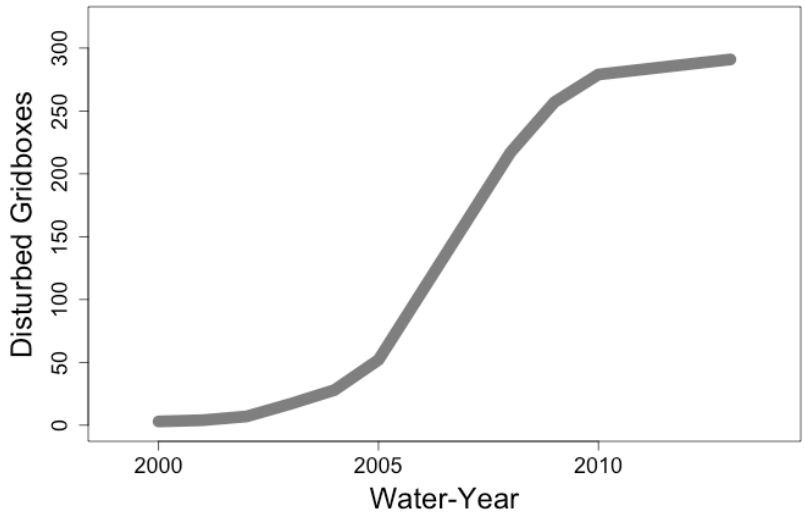

Figure 14. Annual totals of disturbed 1/16° resolution gridboxes in each water-year between 2000 and 2013 shows increased disturbance during the model time period, particularly between 2005 and 2010.

Persistently reduced canopy interception (the amount of precipitation intercepted by the vegetation canopy and subsequently evaporated) in the bark beetle simulations (Figure 15) suggests that leaf area index (LAI) inputs (lower in disturbed simulations) were accurately represented in the model. In each simulation, canopy interception was least during drought in 2002 and greatest in 2011, when precipitation throughout the northern portion of the study domain (where epidemic beetle populations were generally located), in particular snow, was greater than one standard deviation above average (e.g. Knowles et al., 2015b). The mean reduction in canopy interception was 8% from 1.35 mm in the control simulation to 1.24 mm in the beetle simulation.

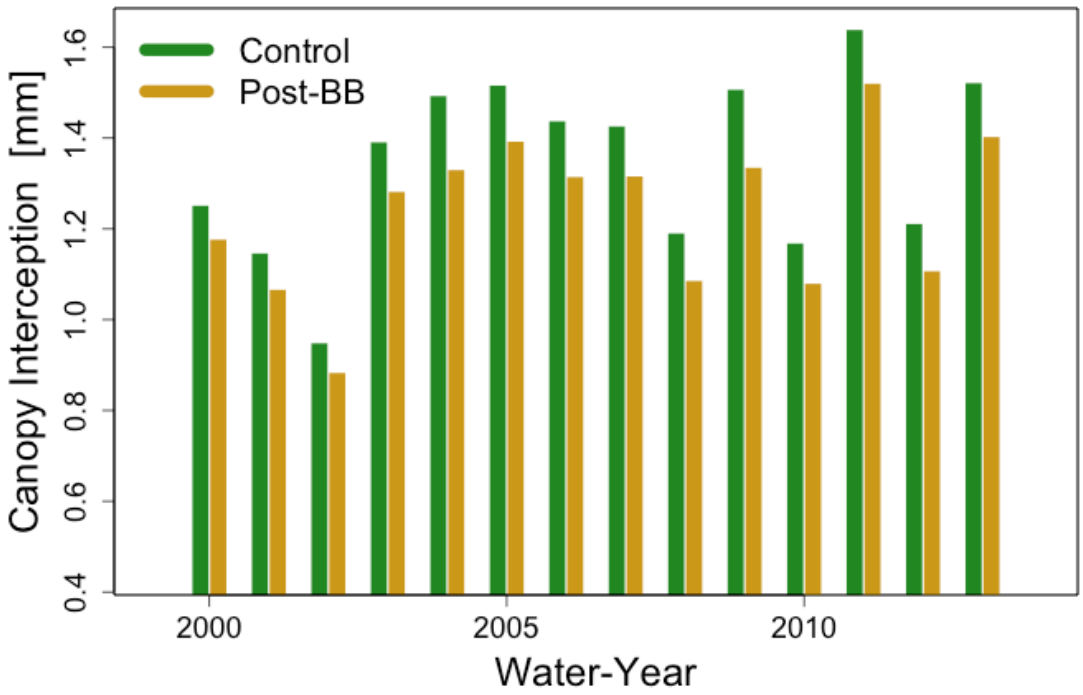

Figure 15. Mean annual (by water-year) canopy intercepted water for control and bark beetle (BB) simulations. Units are mm averaged over the grid cell area.

Total column (i.e., integrated through the entire depth of the soil profile) soil moisture was persistently elevated in model simulations that incorporated the effect of bark beetles, and

the difference between beetle- and control-simulated soil moisture generally increased throughout the study period (Figures 16). Increased soil moisture resulted from reduced canopy interception, which allowed a greater percentage of precipitation to reach the soil surface and subsequently infiltrate. In each simulation, total column soil moisture was greatest in 2011 (wet year) and least in 2002 (dry year).

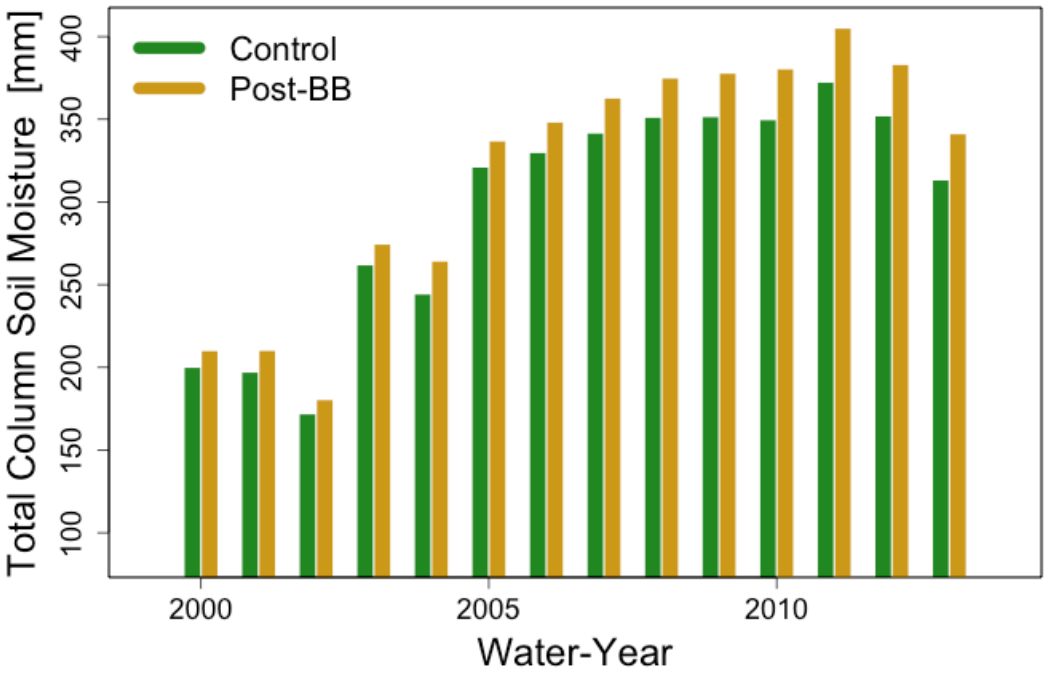

Figure 16. Mean annual (by water-year) total column soil moisture for control and bark beetle (BB) simulations. Units are mm averaged over the grid cell area.

Figure 17 shows the annual cycle of ET by month for control and bark beetle simulations. There was a clear unimodal ET peak during the growing season in both simulations. In the absence of beetle disturbance, the minimum monthly ET was 0.21 mm in December and the maximum monthly ET was 3.3 mm in July. The minimum monthly ET (0.21 mm) was unchanged by incorporating vegetation mortality due to beetle kill but the maximum monthly ET decreased to 3.1 mm. The minimum and maximum ET in the beetle simulations also occurred in

December and July, respectively. Averaged over the whole year, bark beetles decreased ET by 8% from 1.3 mm to 1.2 mm.

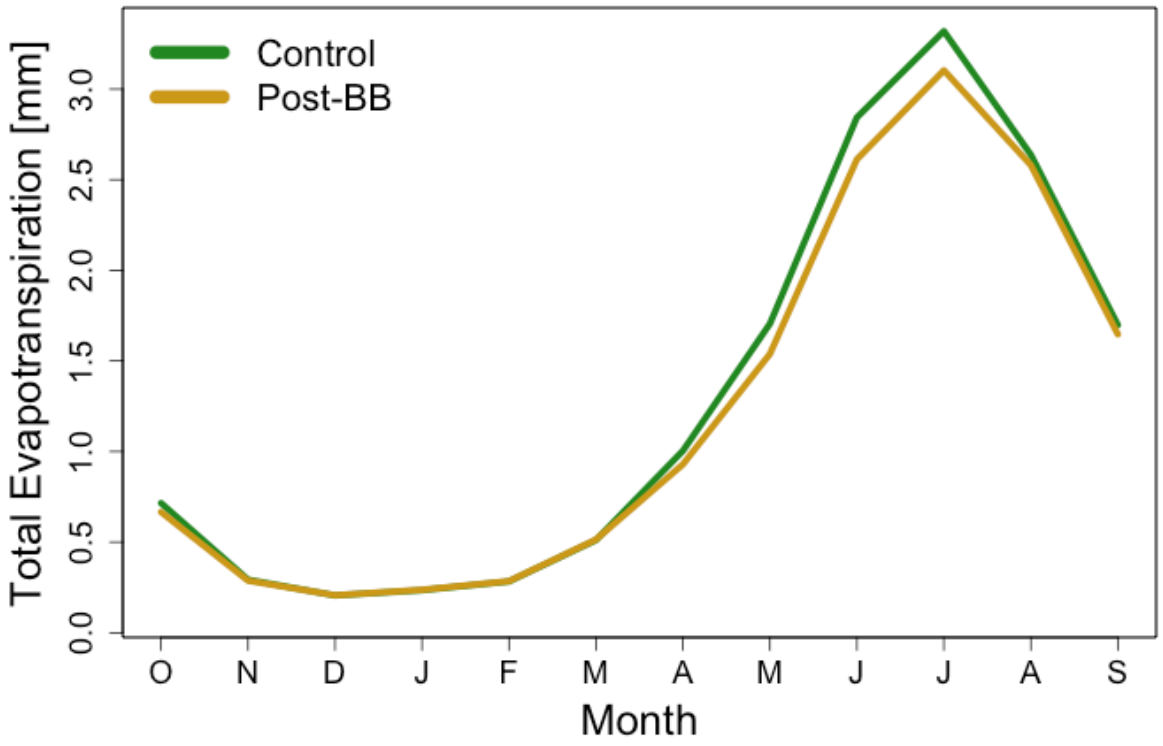

Figure 17. Average annual evapotranspiration (ET) cycle by month for control and bark beetle (BB) simulations between 2000 and 2013. Units are mm averaged over the grid cell area.

Between November and March, there was no difference in ET between the control and beetle simulations (Figure 18). Beginning in April, however, there was evidence of diverging ET, whereby the disturbed ET was reduced relative to the control ET until June, at which point the monthly ET difference became gradually less until the control and beetle ET converged again in November (Figure 18). The maximum difference between the control and beetle ET was 0.22 mm and occurred in June. That the difference between control- and beetle-simulated ET uniquely occurred during the growing season suggests that the principal effect of beetles was to reduce the biotic component of ET i.e., transpiration.

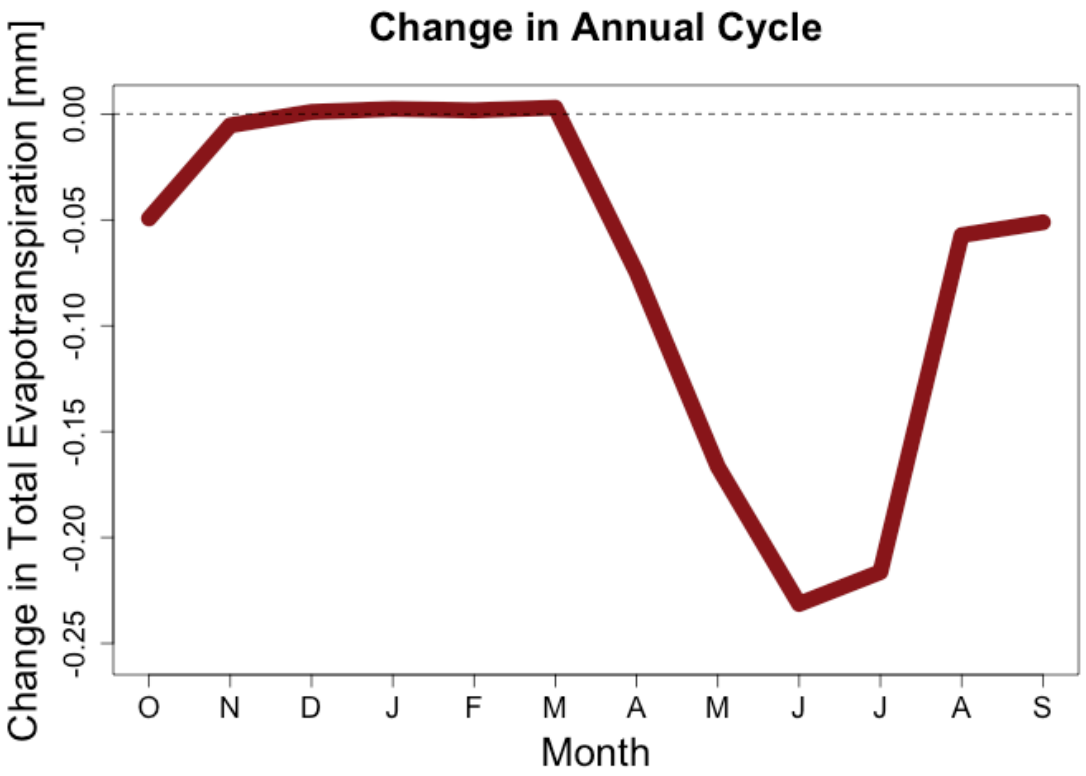

Figure 18. The monthly change in total evapotranspiration (ET) between control and disturbed simulations during the period 2000-2013. A reduction in ET from disturbed areas is evident during the growing season. Units are mm averaged over the grid cell area.

Annually, the total annual ET was always greater in the control relative to the beetle simulations (Figure 19). The minimum total annual ET in both the control and beetle simulations coincided with regional drought in 2002, when the control and beetle total annual ET were 9.3 mm and 9.2 mm, respectively. The maximum total annual control ET was 17.2 mm in 2007, and the maximum total annual beetle ET was 16.3 mm in 2012, which was also a drought year. Over the entire study period, bark beetles decreased the mean total annual ET by 6% from 15.5 mm to 14.6 mm.

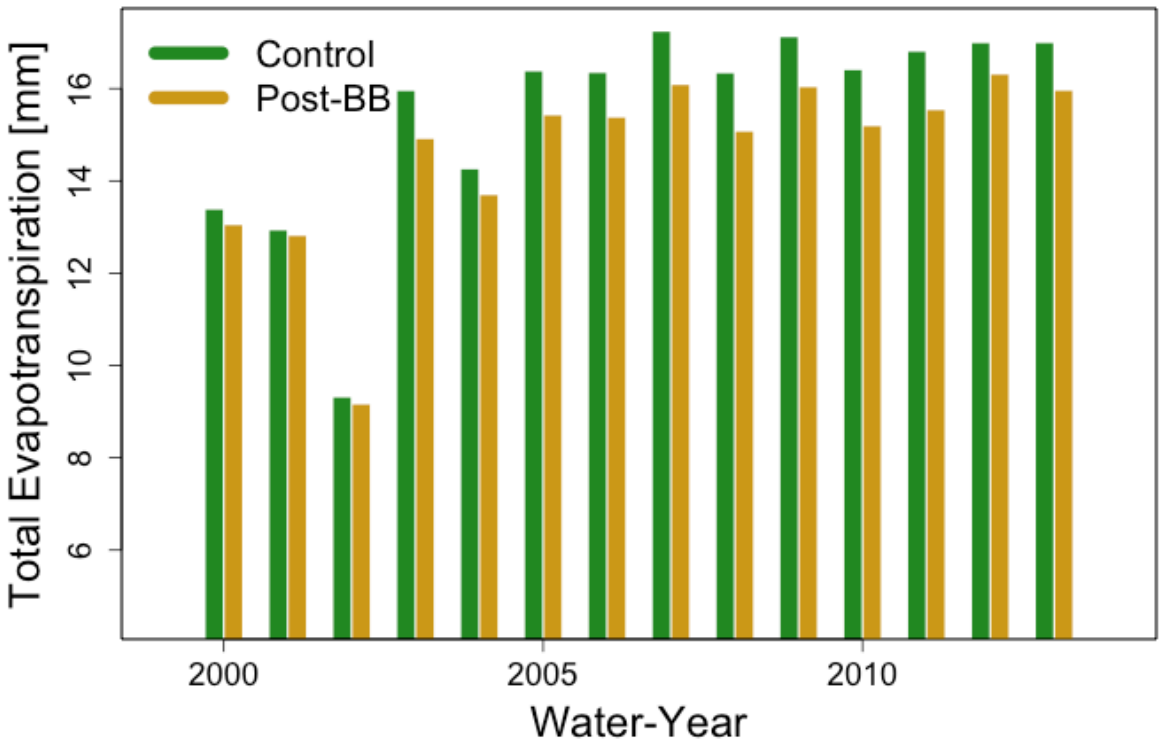

Figure 19. The mean annual (by water-year) evapotranspiration (ET) flux resultant from control and bark beetle (BB) simulations. The ET was persistently decreased in BB relative to control simulations. Units are mm averaged over the grid cell area.

Figure 20 demonstrates how simulated bark beetle disturbance affected total annual ET through time. In general, the total annual beetle ET was depressed by 1 mm or more relative to the control ET beginning in 2005 (Figure 20). The exception to this occurred in 2012, when the difference between the control and beetle ET was 0.7 mm, which was only approximately half the difference from the previous year. Since the 2012 climatology was characterized by widespread drought throughout the Southern Rocky Mountain ecoregion, this suggests the potential for differential effects of drought on ET in the presence or absence of beetle disturbance.

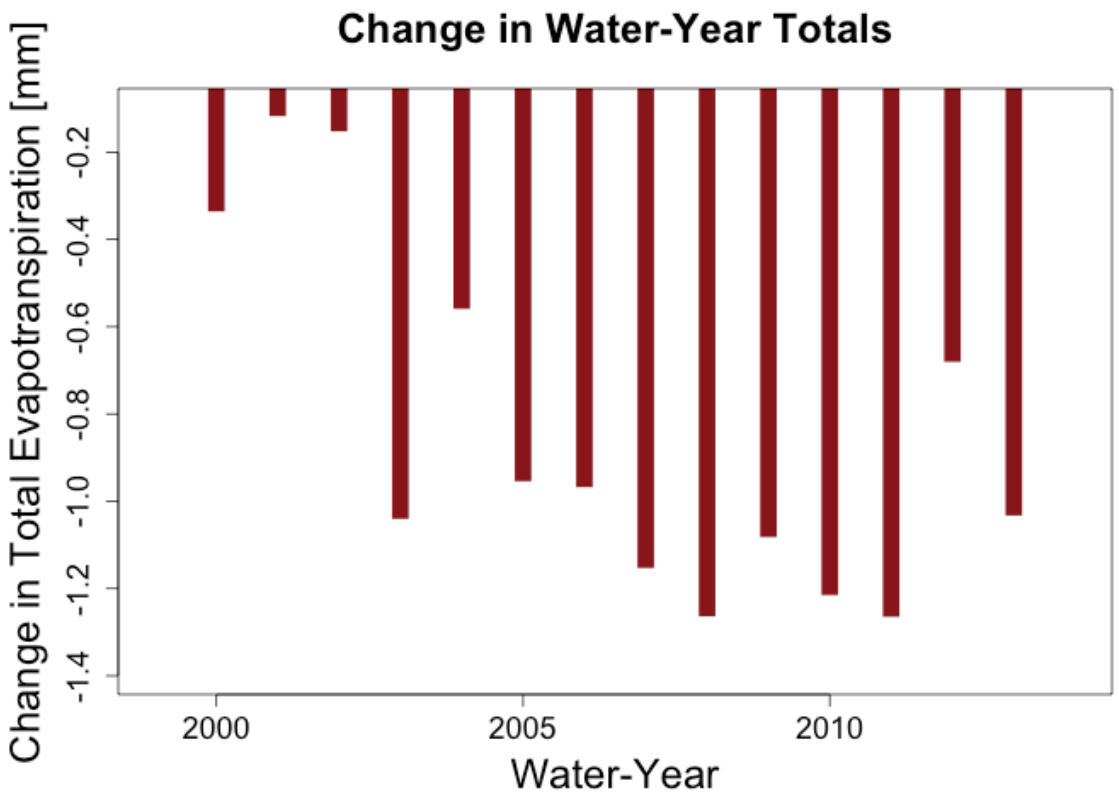

Figure 20. Change in modeled evapotranspiration (ET) from disturbed relative to control simulations by water-year. Negative values demonstrate persistently reduced ET due to beetles. Units are mm averaged over the grid cell area.

Parallels between the average annual transpiration (Figure 21) and ET (Figure 17) cycles indicate that changes in transpiration were the principal contributor to modeled ET reductions as a consequence of beetle disturbance. Similar to ET, there was no significant transpiration difference between control and beetle simulations from November to March when transpiration was negligible, but control transpiration was greater than beetle transpiration during the remainder of the year. The difference between control and beetle transpiration peaked at the same magnitude (0.2 mm) as the maximum difference between control and beetle ET; therefore, reduced transpiration was primarily responsible for observed changes in ET. In July and December, the maximum and minimum mean monthly transpiration fluxes were 2.2 mm and 0.007 mm, respectively, in the control simulation and 2.0 mm and 0.007 mm in the beetle

simulation. Averaged over the whole year, bark beetles had the effect of decreasing transpiration by 8% from 0.70 mm to 0.64 mm.

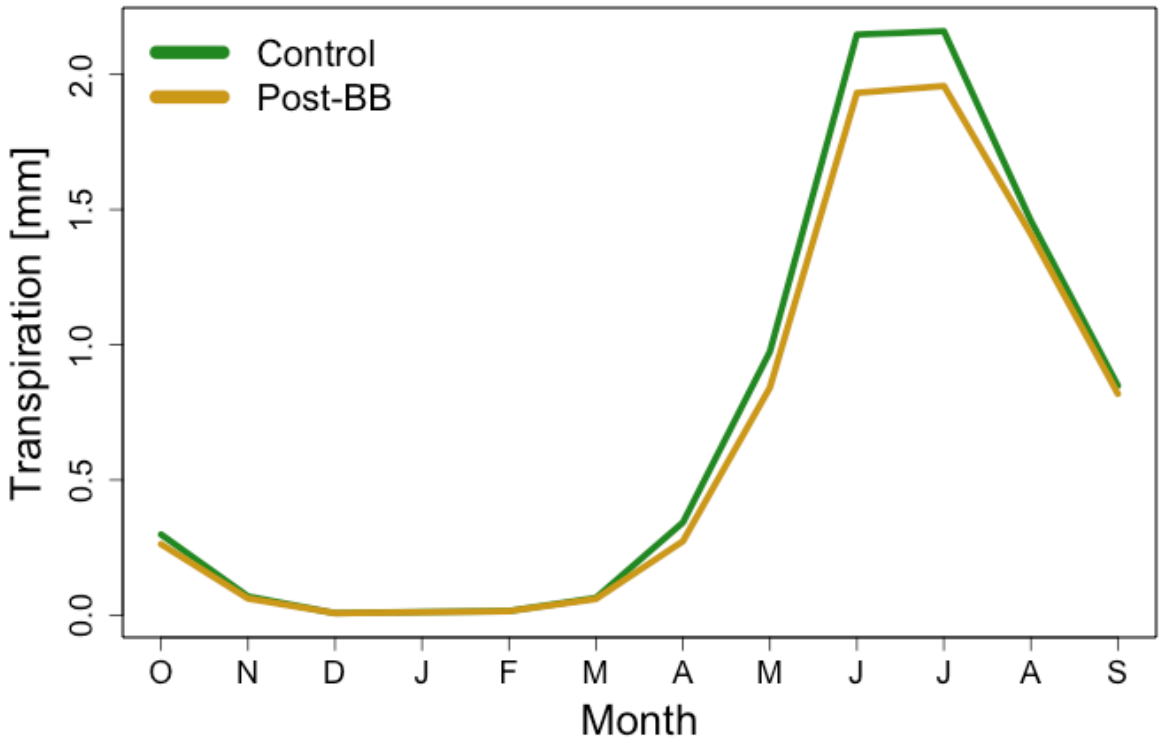

Figure 21. The annual transpiration (T) cycle by month for control and bark beetle (BB) simulations between 2000 and 2013. Units are mm averaged over the grid cell area. Reduced transpiration is evident from disturbed areas during the growing season.

Although the largest absolute transpiration difference between control and beetle simulations occurred in June and July, disturbance had the greatest relative effect on transpiration in April and May (Figure 22). Since this period corresponds to peak snowmelt water availability at many elevations throughout the Southern Rocky Mountain ecoregion (Trujillo & Molotch, 2014), reduced transpiration during this time signals that the model was accurately representing vegetation mortality in the beetle scenario. Monthly transpiration reductions shown by Figure 22 during the winter result from dividing two small numbers and do not reflect meaningful differences in the actual transpiration flux.

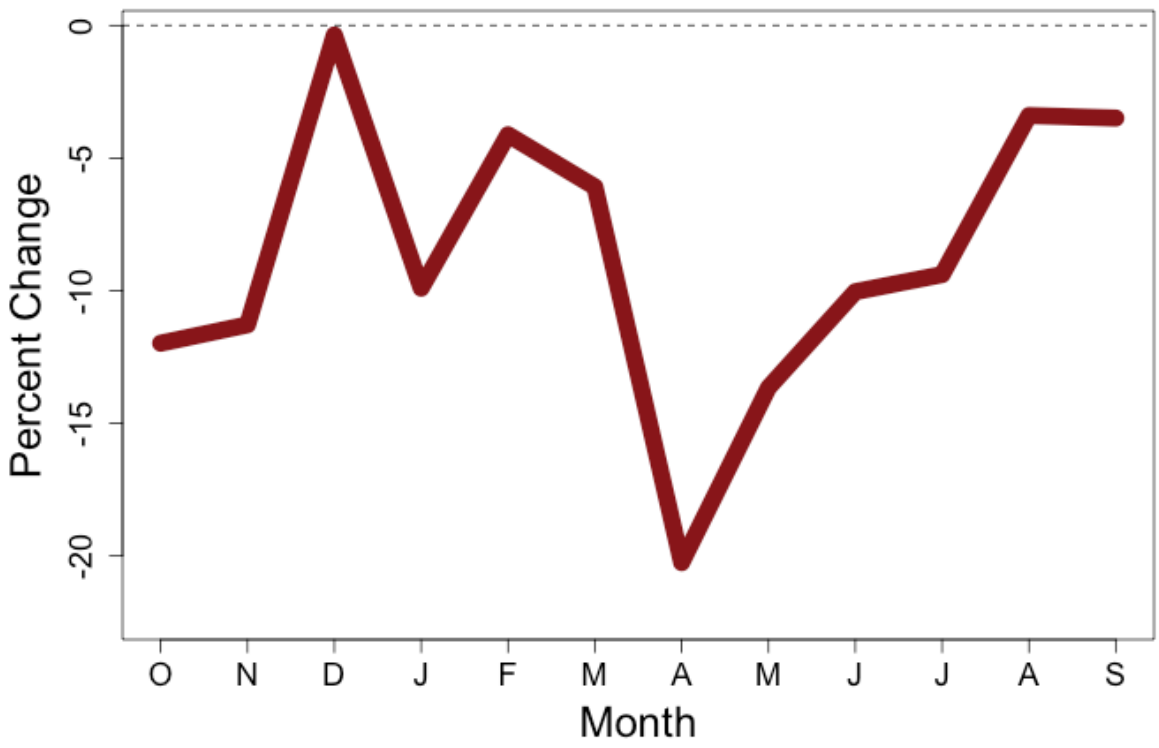

Figure 22. The mean monthly percent change in transpiration between control and disturbed simulations during the period 2000-2013. A reduction in transpiration from disturbed areas is evident during the growing season (apparent changes during winter result from the quotient of two small numbers).

Annually, the total annual transpiration flux was persistently greater in the control relative to the beetle simulations (Figure 23). Similar to ET, the control simulation transpiration peaked in 2007 (10.0 mm), whereas the beetle simulation transpiration peaked in 2012 (9.4 mm). Unexpectedly, this result demonstrates that transpiration, not abiotic evaporation, was responsible for the 2012 ET maximum in the beetle simulation and the corresponding reduced difference between both ET and transpiration during that year. A possible explanation for this is greater soil moisture in the beetle simulation, which could promote transpiration from live trees in areas affected by beetles when soil moisture was limiting to transpiration (i.e. during drought) in undisturbed areas. Both simulations showed a clear transpiration minimum around 3.3 mm

during regional drought conditions in 2002. Overall, bark beetles had the effect of decreasing the mean total annual transpiration flux by 9% from 8.4 mm to 7.6 mm.

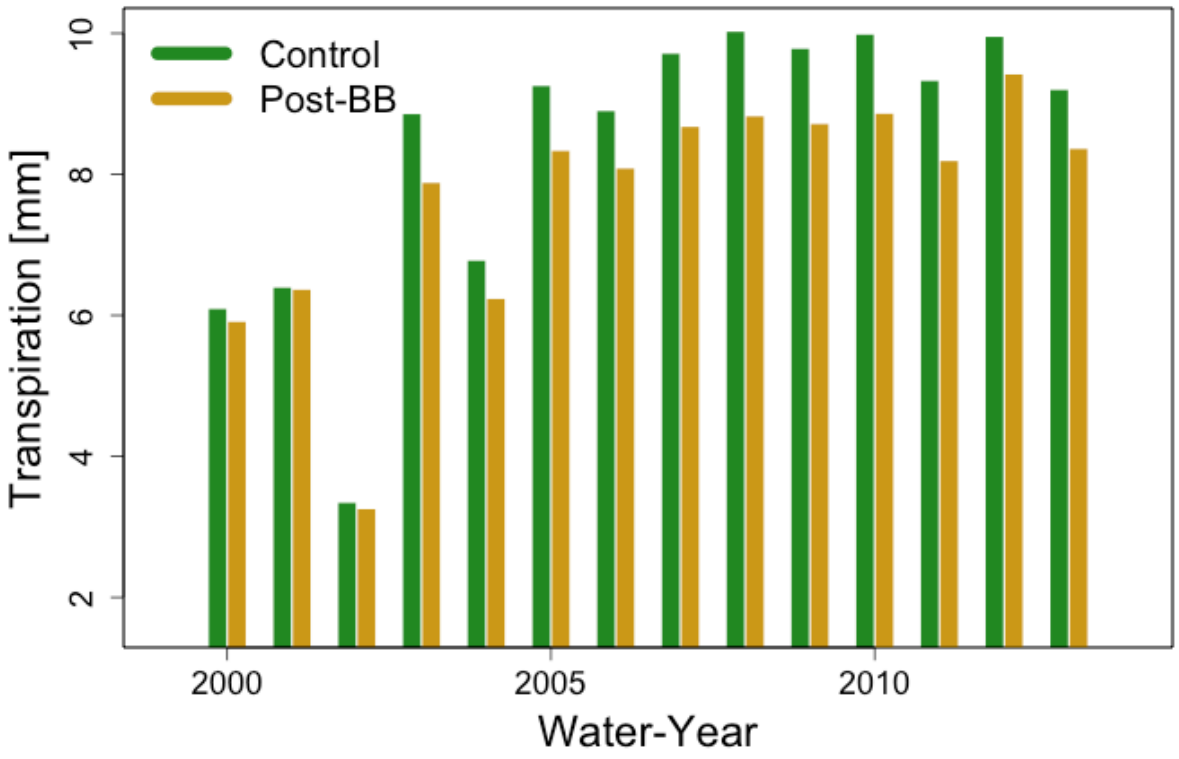

Figure 23. The mean annual (by water-year) transpiration flux resultant from control and bark beetle (BB) simulations. The transpiration flux was persistently depressed in BB relative to control simulations. Units are mm averaged over the grid cell area.

The relative annual transpiration reduction due to bark beetles was greatest in 2011 and least in 2001 (Figure 24), and there was evidence of a step change between 2002 and 2003 when the difference between control- and beetle-simulated transpiration increased by a factor of five from 2% to more than 10%. This was likely due to sampling where transpiration from disturbed areas early in the study period tended to be lower to begin with (Figure 23). After 2002, transpiration was approximately 8% to 12% lower in the beetle relative to the control simulations excepting 2012, when the difference was reduced by the occurrence of the maximum annual transpiration in the beetle simulation (Figure 23).

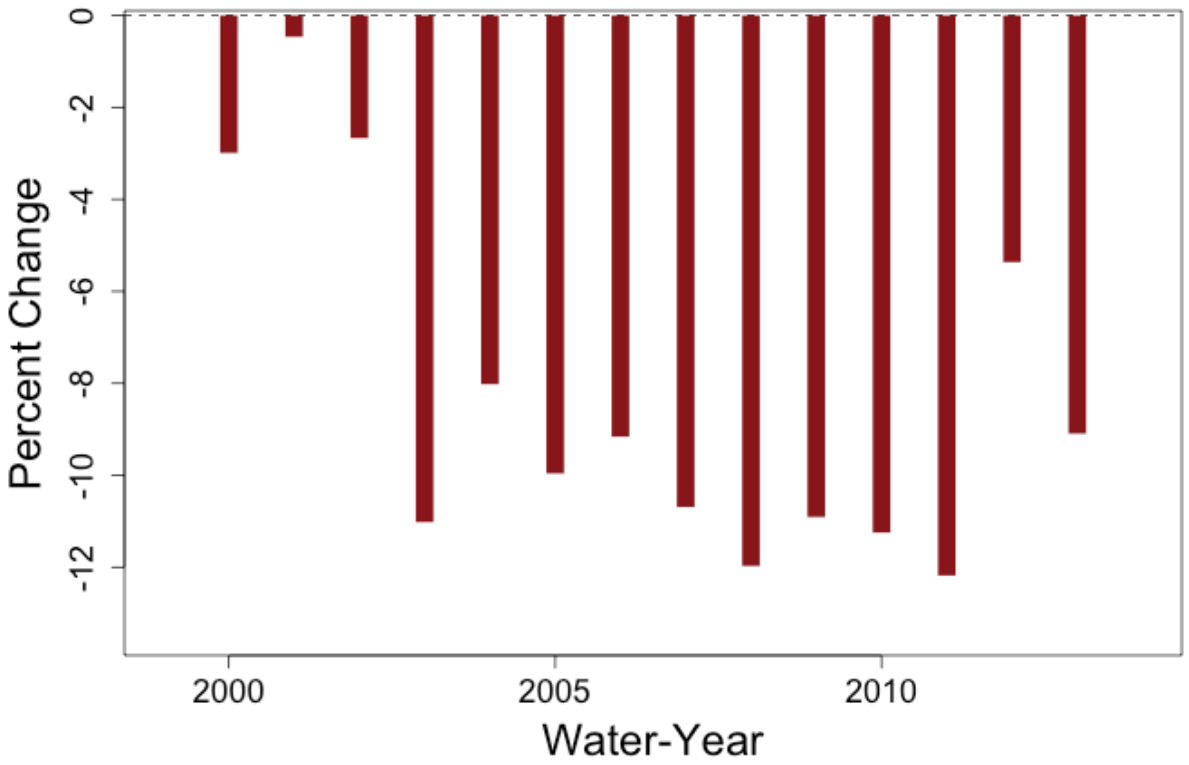

Figure 24. Percent change in modeled transpiration from disturbed relative to control simulations by water-year. Negative values demonstrate reduced transpiration as a result of disturbance in all years. Units are mm averaged over the grid cell area.

Figure 25 integrates the annual cycles of ET (Figure 17) and transpiration (Figure 21) to show the average annual cumulative fluxes from the control and beetle simulations. Specifically, the average cumulative annual ET and transpiration fluxes from the control simulation were 15.5 mm and 8.4 mm, respectively, while the analogous transpiration fluxes were 14.6 mm and 7.6 mm. In this way, there was a 6% reduction in ET and a 10% reduction in transpiration as a result of simulated vegetation mortality due to bark beetles. Multiplying by the average number of control and disturbed grid cells throughout the study period, this corresponds to average annual reductions in ET and transpiration of 25 acre-feet and 22 acre-feet, respectively. Moreover, increasing divergence between control and disturbed simulations throughout the growing season reinforces that most of the change in ET was a result of reduced transpiration from disturbed areas (Figure 25).

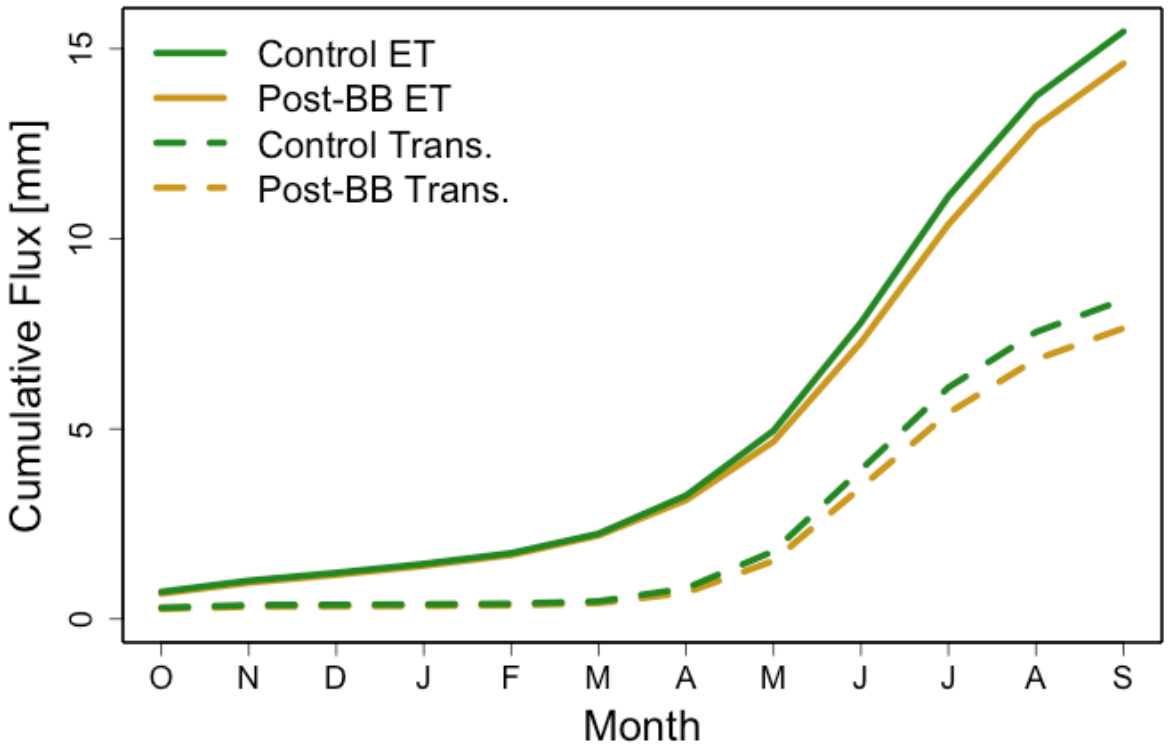

Figure 25. The average cumulative monthly total evapotranspiration (ET) and transpiration (Trans.) fluxes between 2000 and 2013.

The transpiration (T) fraction of total ET (T/ET) was reduced in the bark beetle relative to the control simulation for all years except 2001 (Figure 26). In each simulation, the minimum T/ET was approximately 0.36 during the 2002 drought and the maximum T/ET occurred in 2008 at 0.61 and 0.59 for the control and beetle simulations, respectively. On average, beetles reduced the mean T/ET by 3% from 0.54 to 0.52.

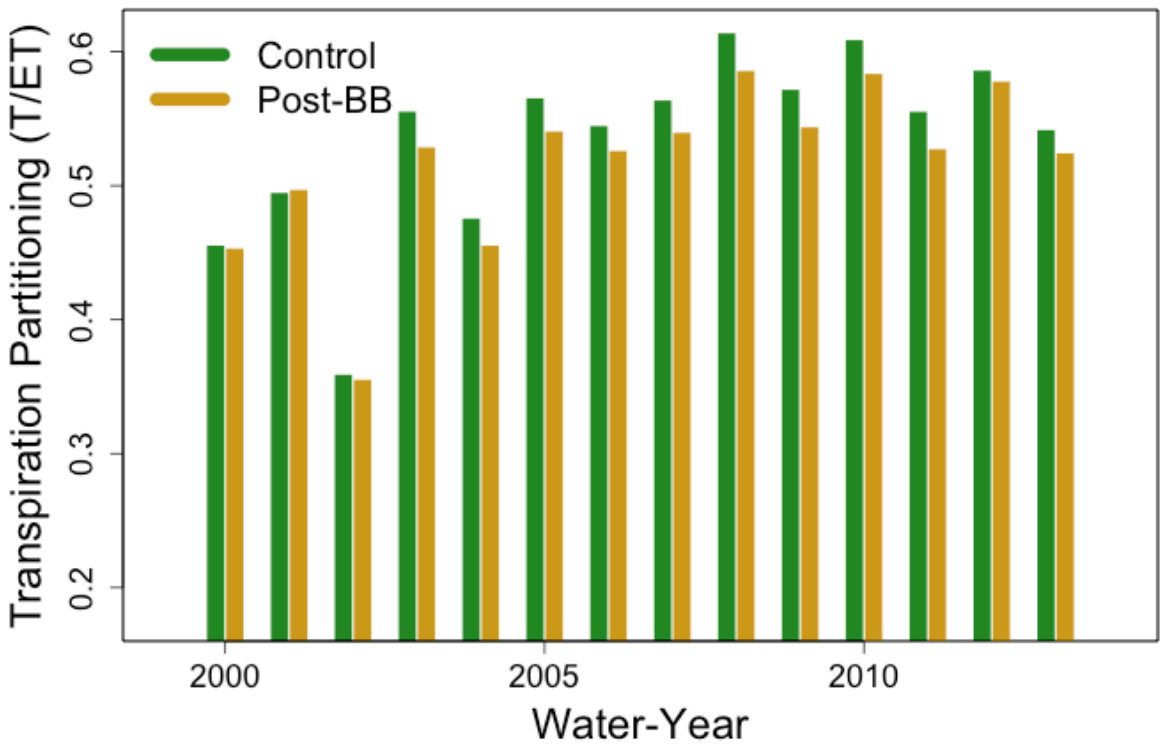

Figure 26. Bark beetle disturbance reduced transpiration as a percentage of ET (T/ET) in all years.

The evaporative fraction (EF) is calculated as the latent heat flux (evaporation) divided by the sum of the latent and sensible heat (temperature) fluxes. In this way, the EF describes the fraction of energy that was partitioned to evaporation versus temperature changes. In general, EF varies with aridity, where EF is higher in more arid systems and lower in less arid systems. Bark beetles decreased the EF in every year relative to the control simulation, which signifies that a lesser percentage of available energy was used to evaporate water (Figure 27). Since meteorological conditions were held constant between model simulations, this indicates less moisture availability and generally more arid conditions in the beetle relative to the control simulation. The EF was greatest in 2011 and least in 2002 in each simulation. Specifically, the maximum and minimum annual EF was 0.23 (i.e. 23% of available energy converted to ET) and

0.69 in the control simulation and 0.22 and 0.62 in the beetle simulation. As a result of beetles, the annual mean EF decreased by 8% from 0.52 to 0.48.

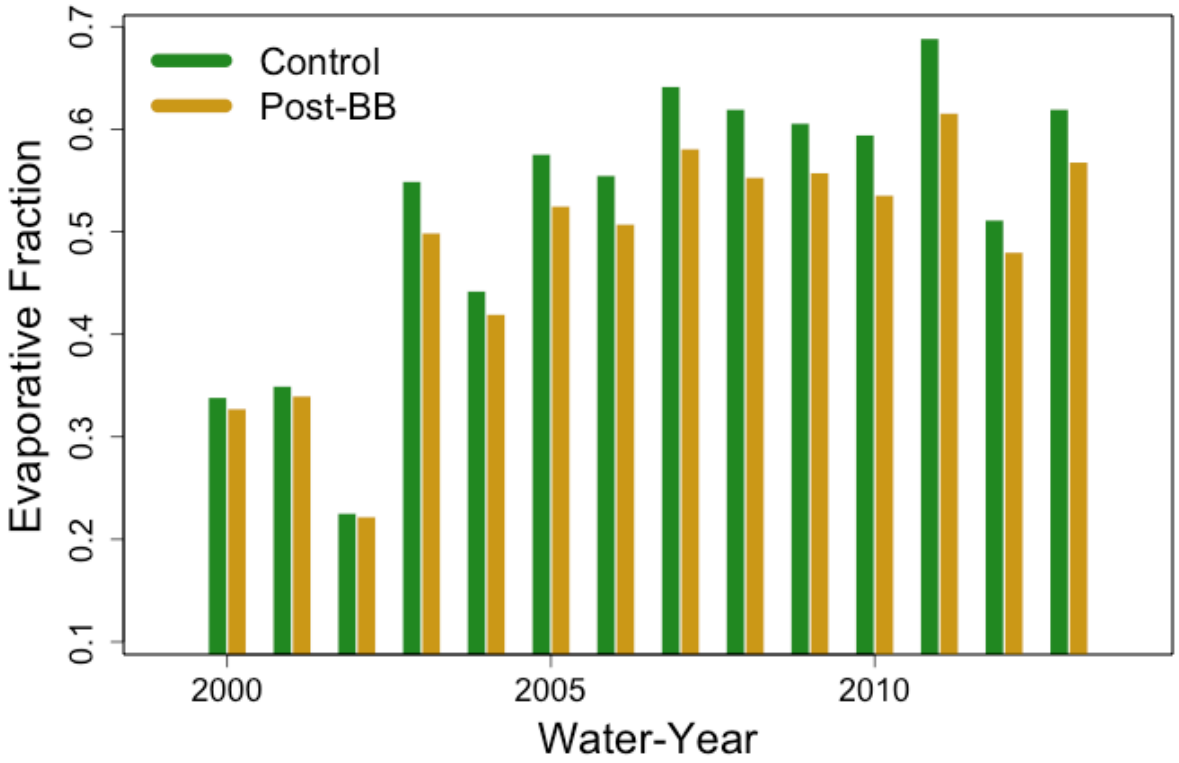

Figure 27. The mean annual (by water-year) modeled evaporative fraction (percentage of available energy translated to evapotranspiration) for control and bark beetle (BB) simulations.

Total annual runoff was higher in the beetle relative to the control simulations (Figure 28). Since the water balance dictates that hydrological inputs of precipitation are balanced by hydrological outputs of ET and stream runoff and/or changes in storage, increased total annual runoff in the presence of beetles resulted from decreased ET due to vegetation mortality. There was clear runoff peak in 2011 when above-average precipitation resulted in 15.0 mm and 13.6 mm runoff in the beetle and control simulations, respectively. Regardless of disturbance, very low runoff between 2000 and 2002 can be interpreted as a sampling artifact where epidemic beetle populations were uniquely present in relatively dry areas during that time. On average, bark beetles increased total annual runoff by 9% from 6.3 mm to 6.9 mm.

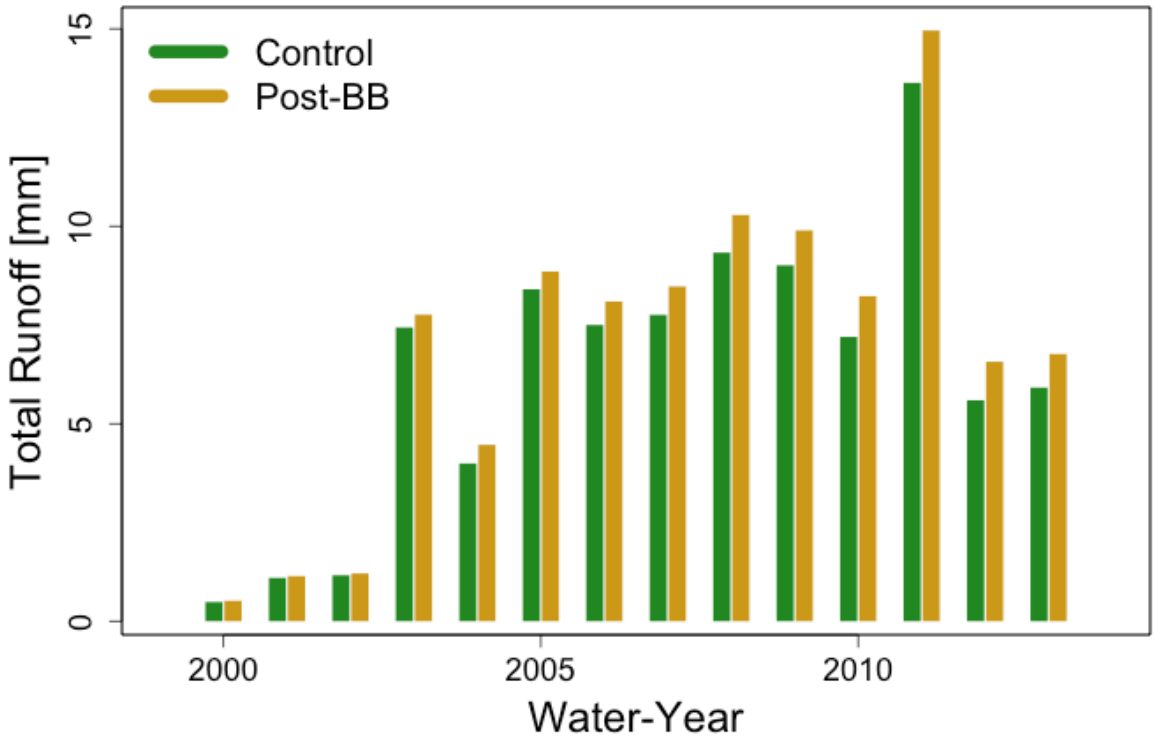

Figure 28. Total annual (by water-year) modeled runoff for control and bark beetle (BB)-affected areas throughout the Southern Rocky Mountain ecoregion. Units are mm averaged over the grid cell area.

There was a general increasing trend in the annual runoff difference between disturbed and undisturbed areas beginning in 2005 with the onset of widespread beetle disturbance (Figure 29). Specifically, the difference in total annual runoff between the beetle and control simulations was greatest in 2012 and least in 2001. That the runoff difference was greatest in 2012 (when the difference between the both the control and beetle ET and transpiration fluxes was relatively diminished due to higher fluxes in the beetle scenario; Figures 19, 23) demonstrates the potential for synoptic meteorological variability to modify the effect of disturbance on hydrological partitioning between runoff and ET i.e., the magnitude of the runoff difference was greater than the magnitude of the ET difference. In this case, although 2012 was a low snow year throughout the northern (beetle-affected) portion of the study domain, there was above average precipitation during the summer. Consequently, relatively more runoff in the beetle versus the control

simulation during 2012 could reflect greater runoff sensitivity to the seasonality and/or phase of precipitation in undisturbed compared to disturbed areas.

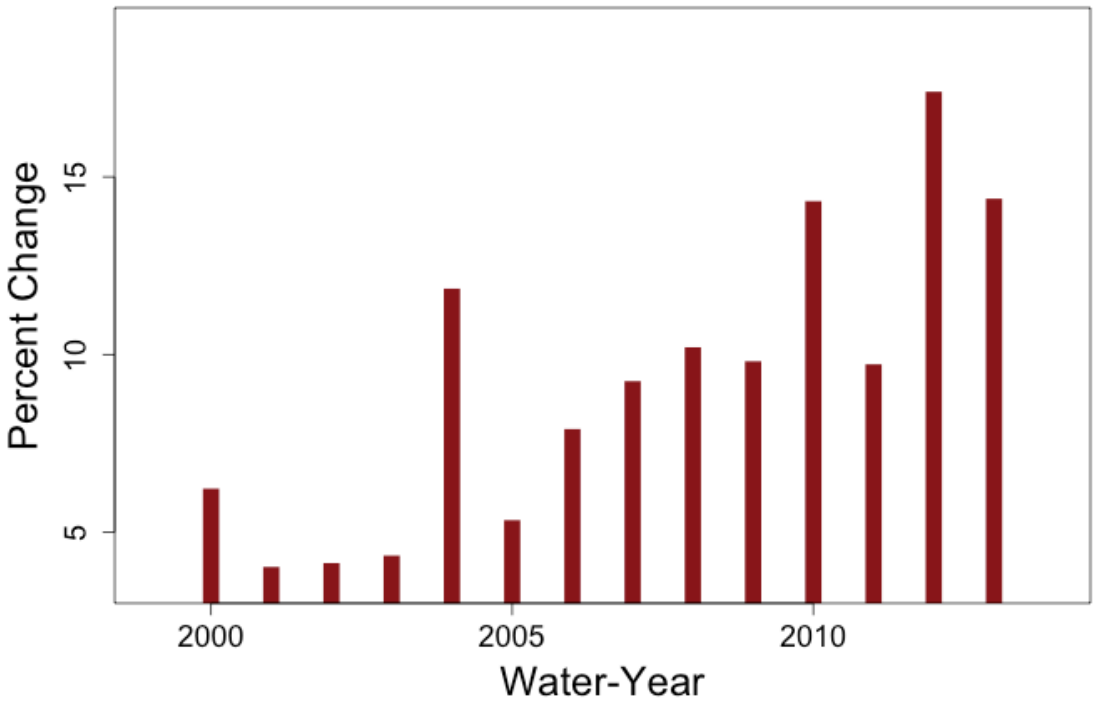

Figure 29. Percent change in modeled runoff from disturbed relative to control areas by water-year.

From a water resources perspective, the annual modeled hydrological cycles of ET, transpiration, and runoff can be expressed in volumetric units by multiplying the monthly values by the corresponding number of grid cells that have been disturbed. In this way, the cumulative volumetric ET between 2000 and 2013 was 979 kaf (thousand acre-feet) in the control simulation, compared to 917 kaf in the beetle simulation (Figure 30a). The equivalent cumulative volumetric control and beetle transpiration fluxes were 560 kaf and 504 kaf (Figure 30a), and the control and beetle runoff fluxes were 478 kaf and 532 kaf, respectively (Figure 30b). Accordingly, the cumulative difference between the volumetric ET, transpiration, and runoff fluxes was 62 kaf (6% decrease), 56 kaf (10% decrease), and 54 kaf (11% increase).

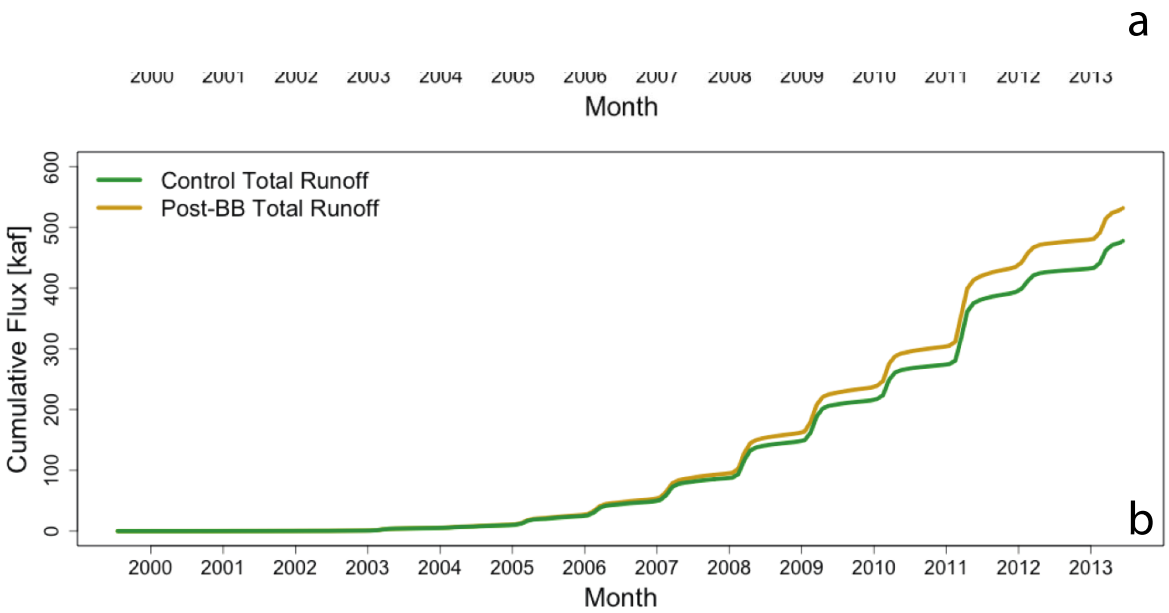

Figure 30. Cumulative volumetric (a) evapotranspiration (ET), transpiration (Trans.) and (b) runoff from control and beetle simulations between 2000 and 2013. Units are thousand acre-feet (kaf).

IV. PRINCIPAL FINDINGS, CONCLUSIONS, AND RECOMMENDATIONS

The results of this study highlight several key ways in which bark beetles influence hydrological partitioning between evaporation, transpiration, and streamflow in the southern Rocky Mountains:

1. Multi-scale remote sensing analyses from control and disturbed areas demonstrated statistically significant 9% (ecoregion) and 13% (focus areas) reductions in growing season ET due to vegetation mortality from bark beetles between 2000 and 2013.

2. Comparison of eddy covariance measurements at GLEES, WY (beetles) and Niwot Ridge, CO (control) showed that the post-disturbance growing season ET was an average of 102 mm (28%) less at GLEES compared to Niwot Ridge (the pre-disturbance GLEES ET had been higher than Niwot Ridge). There was a statistically significant decreasing growing season ET trend at GLEES but not at Niwot Ridge.
3. There was a statistically significant 10% decrease in the modeled (from eddy covariance) T/ET at GLEES between 2005 and 2017 (no change at Niwot Ridge).
4. There was a statistically significant positive relationship between growing season ET and T at GLEES (no relationship at Niwot Ridge), suggesting that changes in T/ET were responsible for observed changes in ET.
5. A hydrological model (VIC) simulated reduced canopy interception and increased soil moisture as a result of bark beetle disturbance. This indicates that prescribed changes in leaf area index and stomatal conductance were applied correctly by the model.
6. The hydrological model demonstrated a 6% reduction in ET, a 9% reduction in transpiration, a 3% reduction in the transpiration fraction of ET (T/ET), and an 8% reduction in the evaporative fraction as a result of bark beetles. Decreased EF is generally indicative of a more arid environment.
7. The eddy covariance- and VIC-modeled T/ET each decreased by 0.02 in the presence of epidemic bark beetle populations.
8. Modeled stream runoff increased by 9% as a result of both decreased ET (more water available for runoff) and increased soil moisture (precipitation inputs more readily converted to runoff due to higher hydraulic conductivity; Barnhart et al., 2016).

9. Bark beetles reduced the cumulative modeled ET and transpiration fluxes by 62,000 acre-feet and 56,000 acre-feet, respectively, throughout the southern Rocky Mountain ecoregion between 2000 and 2013. There was a corresponding cumulative stream runoff increase of 54,000 acre-feet during the same period.
10. Direct measurements of transpiration via the sapflow method would be useful to independently validate the eddy covariance- and VIC-modeled T/ET values in this study. Our results also suggest that future investigation into the transpiration and ET responses to drought from control and beetle-disturbed areas could be fruitful. Follow-up research focused on the effect of forest regrowth on hydrologic partitioning is strongly recommended.

V. SUMMARY

Bark beetles reached epidemic populations throughout many areas of the Southern Rocky Mountain ecoregion during the mid 2000s, resulting in widespread forest mortality with variable and potentially interactive consequences on hydrological partitioning (Buma & Livneh, 2017; Edburg et al., 2012). Based on physical principles and previous work (Biederman et al., 2014; 2015), we hypothesized decreased evapotranspiration (ET) as a result of this scenario, but also increased abiotic evaporation that could moderate the effect of decreased biotic transpiration on the total ET flux. Given that changes in ET affect both surface water and groundwater recharge (Maxwell & Condon, 2016; Ukkola et al., 2015), there are major implications for water resources in the Rocky Mountains associated with any perturbation to seasonal or annual hydrological partitioning due to bark beetles. Accordingly, this study used a multi-scale observational approach coupled to a hydrological model to evaluate the impact of bark beetles on both

transpiration and total evapotranspiration within the context of streamflow and the hydrological cycle.

Our results at the ecosystem (1 km^2), focus area (10^2 km^2), and ecoregion (10^5 km^2) scale indicate that bark beetles significantly decreased growing season evapotranspiration and that this reduction was generally commensurate with decreased transpiration i.e., we did not detect a significant compensatory abiotic evaporation response. Instead, a hydrological model demonstrated increased soil moisture and streamflow runoff, suggesting not only that more precipitation was partitioned to streamflow, but also that precipitation may have been more readily converted to streamflow as a result of increased subsurface hydrological conductivity. Our research design included simultaneous multi-scale comparison of disturbed versus undisturbed areas, which allowed us to isolate the effect of beetles on transpiration and ET. As a result, we can conclusively attribute the trends reported herein to bark beetles rather than meteorological, topographical, or sampling variability.

Throughout the Southern Rocky Mountain ecoregion, our modeling analysis shows that bark beetles decreased the cumulative ET flux by 62,000 acre-feet and increased the corresponding stream runoff flux by 54,000 acre-feet between 2000 and 2013. For comparison, this represented an 11% increase in stream runoff relative to the control simulation, and 54,000 acre-feet is approximately equivalent to the annual water usage by 250,000 Colorado citizens or 10% of Colorado's estimated 2050 water deficit (Colorado's Water Plan, 2015). However, since beetle-induced vegetation mortality in Colorado has been declining since 2008 (Mountain pine beetle) or 2012 (spruce beetle) (Colorado State Forest Service, 2017), increased stream runoff from beetles cannot be counted as a reliable water resource in the future. We therefore identify future research on the effects of forest regrowth on hydrological partitioning as an important

research priority. In the meantime, we recommend that water managers and/or forecasters take advantage of the multi-scale results presented herein to accurately interpret the magnitude of the beetle effect on current hydrological observations.

VI. REFERENCES

Aubinet, M., Grelle, A., Ibrom, A., Rannik, Ü., Moncrieff, J. B., Foken, T., et al. (2000). Estimates of the annual net carbon and water exchange of forests: the EUROFLUX methodology. *Advances in Ecological Research*, *30*, 113–175.

Baldocchi, D. D., Falge, E., Gu, L., Olson, R., Hollinger, D., Running, S., et al. (2001). FLUXNET: a new tool to study the temporal and spatial variability of ecosystem-scale carbon dioxide, water vapor, and energy flux densities. *Bulletin of the American Meteorological Society*, *82*(11), 2415–2434.

Barnhart, T. B., Molotch, N. P., Livneh, B., Harpold, A. A., Knowles, J. F., & Schneider, D. (2016). Snowmelt rate dictates streamflow. *Geophysical Research Letters*, *43*(15), 8006–8016. http://doi.org/10.1002/2016GL069690

Beer, C., Ciais, P., Reichstein, M., Baldocchi, D., Law, B. E., Papale, D., et al. (2009). Temporal and among-site variability of inherent water use efficiency at the ecosystem level. *Global Biogeochemical Cycles*, *23*(2), GB2018. http://doi.org/10.1029/2008GB003233

Berkelhammer, M., Noone, D. C., Wong, T. E., Burns, S. P., Knowles, J. F., Kaushik, A., et al. (2016). Convergent approaches to determine an ecosystem's transpiration fraction. *Global Biogeochemical Cycles*, *30*, 933–951. http://doi.org/10.1002/2016GB005392

Biederman, J. A., Harpold, A. A., Gochis, D. J., Ewers, B. E., Reed, D. E., Papuga, S. A., & Brooks, P. D. (2014). Increased evaporation following widespread tree mortality limits streamflow response. *Water Resources Research*, *50*(7), 5395–5409. http://doi.org/10.1002/2013WR014994

Biederman, J. A., Somor, A. J., Harpold, A. A., Gutmann, E. D., Breshears, D. D., Troch, P. A., et al. (2015). Recent tree die-off has little effect on streamflow in contrast to expected increases from historical studies. *Water Resources Research*, *51*(12), 9775–9789. http://doi.org/10.1002/2015WR017401

Buma, B., & Livneh, B. (2017). Key landscape and biotic indicators of watersheds sensitivity to forest disturbance identified using remote sensing and historical hydrography data. *Environmental Research Letters*, *12*(7). http://doi.org/10.1088/1748-9326/aa7091

Burns, S. P., Maclean, G. D., Blanken, P. D., Oncley, S. P., Semmer, S. R., & Monson, R. K. (2016). The Niwot Ridge Subalpine Forest US-NR1 AmeriFlux site - Part 1: Data acquisition and site record-keeping. *Geoscientific Instrumentation, Methods and Data Systems*, *5*(2), 451–471. http://doi.org/10.5194/gi-5-451-2016

Colorado State Forest Service. (2017). 2017 Report on the Health of Colorado's Forests: Meeting the Challenge of Dead and At-Risk Trees. https://csfs.colostate.edu/media/sites/22/2018/02/2017_ForestHealthReport_FINAL.pdf

Colorado's Water Plan: Collaborating on Colorado's Water Future. (2015). Chapter 5: Water Demands. https://www.colorado.gov/pacific/sites/default/files/CWP2016.pdf

Commission for Environmental Cooperation (CEC). (1997). Ecological Regions of North America: Toward a Common Perspective, Montreal, Que., Canada.

Cook, E. R., Woodhouse, C. A., Eakin, C. M., Meko, D. M., & Stahle, D. W. (2004). Long-term aridity changes in the western United States. *Science*, *306*(5698), 1015–1018. http://doi.org/10.1126/science.1102586

Edburg, S. L., Hicke, J. A., Brooks, P. D., Pendall, E. G., Ewers, B. E., Norton, U., et al. (2012). Cascading impacts of bark beetle-caused tree mortality on coupled biogeophysical and biogeochemical processes. *Frontiers in Ecology and the Environment*, *10*(8), 416–424. http://doi.org/10.1890/10173

Frank, J. M., Massman, W. J., Ewers, B. E., Huckaby, L. S., & Negron, J. F. (2014). Ecosystem CO2/H2O fluxes are explained by hydraulically limited gas exchange during tree mortality from spruce bark beetles. *Journal of Geophysical Research: Biogeosciences*, *119*, 1195–1215. http://doi.org/10.1002/2013JG002597

Hicke, J. A., Allen, C. D., Desai, A. R., Dietze, M. C., Hall, R. J., Hogg, E. H., et al. (2012). Effects of biotic disturbances on forest carbon cycling in the United States and Canada. *Global Change Biology*, *18*, 7–34. http://doi.org/10.1111/j.1365-2486.2011.02543.x

Homer, C., Huang, C., Yang, L., Wylie, B., & Coan, M. (2004). Development of a 2001 National Land-Cover Database for the United States. *Photogrammetric Engineering & Remote Sensing*, *70*(7), 829–840. http://doi.org/10.14358/PERS.70.7.829

Huxman, T. E., Wilcox, B. P., Breshears, D. D., Scott, R. L., Snyder, K. A., Small, E. E., et al. (2005). Ecohydrological implications of woody plant encroachment. *Ecology*, *86*(2), 308–319. http://doi.org/10.1890/03-0583

Knowles, J. F., Burns, S. P., Blanken, P. D., & Monson, R. K. (2015a). Fluxes of energy, water, and carbon dioxide from mountain ecosystems at Niwot Ridge, Colorado. *Plant Ecology & Diversity*, *8*(5-6), 663–676. http://doi.org/10.1080/17550874.2014.904950

Knowles, J. F., Harpold, A. A., Cowie, R., Zeliff, M., Barnard, H. R., Burns, S. P., et al. (2015b). The relative contributions of alpine and subalpine ecosystems to the water balance of a mountainous, headwater catchment. *Hydrological Processes*, *29*(22), 4794–4808. http://doi.org/10.1002/hyp.10526

Kool, D., Agam, N., Lazarovitch, N., Heitman, J. L., Sauer, T. J., & Ben-Gal, A. (2014). A review of approaches for evapotranspiration partitioning. *Agricultural and Forest Meteorology*, *184*, 56–70. http://doi.org/10.1016/j.agrformet.2013.09.003

Liang, X., Lettenmaier, D. P., Wood, E. F., & Burges, S. J. (1994). A simple hydrologically based model of land surface water and energy fluxes for general circulation models., *Journal of Geophysical Research: Biogeosciences*, *99*(D7), 14415–14428, http://doi.org/10.1029/94JD00483

Livneh, B., Rosenberg, E. A., Lin, C., Nijssen, B., Mishra, V., Andreadis, K. M., & Lettenmaier, D. P. (2013). A long-term hydrologically based dataset of land surface fluxes and states for the conterminous United States: Update and extensions. *Journal of Climate*, *26*(23), 9384–9392. http://doi.org/10.1175/JCLI-D-12-00508.1

Livneh, B., Bohn, T. J., Pierce, D. W., Munoz-Arriola, F., Nijssen, B., Vose, R., & Brekke, L. (2015). A spatially comprehensive, hydrometeorological data set for Mexico, the US, and Southern Canada 1950-2013. *Scientific Data*, *2*, http://doi.org/10.1038/sdata.2015.42

Maxwell, R. M., & Condon, L. E. (2016). Connections between groundwater flow and transpiration partitioning. *Science*, *353*(6297), 377–380. http://doi.org/10.1126/science.aaf8589

Meddens, A. J. H., Hicke, J. A., & Ferguson, C. A. (2012). Spatiotemporal patterns of observed bark beetle-caused tree mortality in British Columbia and the western United States. *Ecological Applications*, *22*(7), 1876–1891. http://doi.org/10.1890/11-1785.1

Monteith, J. L. (1973). Principles of Environmental Physics, Edward Arnold, London

Moore, D. J., Trahan, N. A., Wilkes, P., Quaife, T., Stephens, B. B., Elder, K., et al. (2013). Persistent reduced ecosystem respiration after insect disturbance in high elevation forests. *Ecology Letters*, *16*, 731–737.

Mu, Q. Z., Zhao, M. S., & Running, S. W. (2011). Improvements to a MODIS global terrestrial evapotranspiration algorithm. *Remote Sensing of Environment*, *115*(8), 1781–1800. http://doi.org/10.1016/j.rse.2011.02.019

Myneni, R., Knyazikhin, Y., & Park, T. (2015). *MOD15A2H MODIS/Terra Leaf Area Index/FPAR 8-Day L4 Global 500m SIN Grid V006* [Data set]. NASA EOSDIS Land Processes DAAC. http://doi.org/10.5067/MODIS/MOD15A2H.006R

Nijssen, B., Lettenmaier, D. P., Liang, X., Wetzel, S. W., & Wood, E. F. (1997). Streamflow simulation for continental-scale river basins. *Water Resources Research*, *33*(4), 711–724. http://doi.org/10.1029/96WR03517

Nijssen, B., Schnur, R., & Lettenmaier, D. P. (2001). Global retrospective estimation of soil moisture using the variable infiltration capacity land surface model. *Journal of Climate*, *14*(8), 1790–1808. http://doi.org/10.1175/1520-0442(2001)014,1790:GREOSM.2.0.CO;2

Oke, T. R. (1997). Boundary Layer Climates, 2nd Edition. Routledge Publishing, New York

Raffa, K. F., Aukema, B. H., Bentz, B. J., Carroll, A. L., Hicke, J. A., & Turner, M. G. (2008). Cross-scale drivers of natural disturbances prone to anthropogenic amplification: the dynamics of bark beetle eruptions. *BioScience*, *58*(6), 501–517.

Reichstein, M., Falge, E., Baldocchi, D., Papale, D., Aubinet, M., Berbigier, P., et al. (2005). On the separation of net ecosystem exchange into assimilation and ecosystem respiration: review and improved algorithm. *Global Change Biology*, *11*, 1424–1439. http://doi.org/10.1111/j.1365-2486.2005.001002.x

Running, S., Mu, Q., Zhao, M. (2017). *MOD16A2 MODIS/Terra Net Evapotranspiration 8-Day L4 Global 500m SIN Grid V006* [Data set]. NASA EOSDIS Land Processes DAAC. http://doi.org/10.5067/MODIS/MOD16A2.006

Speckman, H. N., Frank, J. M., Bradford, J. B., Miles, B. L., Massman, W. J., Parton, W. J., & Ryan, M. G. (2014). Forest ecosystem respiration estimated from eddy covariance and chamber measurements under high turbulence and substantial tree mortality from bark beetles. *Global Change Biology*, *21*(2), 708–721. http://doi.org/10.1111/gcb.12731

Sterling, S. M., Ducharne, A., & Polcher, J. (2012). The impact of global land-cover change on the terrestrial water cycle. *Nature Climate Change*, *3*(4), 385–390. http://doi.org/10.1038/nclimate1690

Trujillo, E., & Molotch, N. P. (2014). Snowpack regimes of the Western United States. *Water Resources Research*, *50*(7), 5611–5623. http://doi.org/10.1002/2013WR014753

Turnipseed, A. A., Blanken, P. D., Anderson, D. E., & Monson, R. K. (2002). Energy budget above a high-elevation subalpine forest in complex topography. *Agricultural and Forest Meteorology*, *110*, 177–201.

Ukkola, A. M., Prentice, I. C., Keenan, T. F., van Dijk, A. I. J. M., Viney, N. R., Myneni, R. B., & Bi, J. (2015). Reduced streamflow in water-stressed climates consistent with CO2 effects on vegetation. *Nature Climate Change*, *6*(1), 75–78. http://doi.org/10.1038/nclimate2831

United States (US) Environmental Protection Agency (EPA). (2010). Level III Ecoregions of the Continental United States. U.S. EPA National Health and Environmental Effects Research Laboratory, Map M-1, Various Scales, Corvallis, Oreg.

Viviroli, D., Archer, D. R., Buytaert, W., Fowler, H. J., Greenwood, G. B., Hamlet, A. F., et al. (2011). Climate change and mountain water resources: overview and recommendations for research, management and policy. *Hydrology and Earth System Sciences*, *15*(2), 471–504. http://doi.org/10.5194/hess-15-471-2011

Zhou, S., Yu, B., Huang, Y., & Wang, G. (2014). The effect of vapor pressure deficit on water use efficiency at the subdaily time scale. *Geophysical Research Letters*, *41*(14), 5005–5013. http://doi.org/10.1002/2014GL060741